IEEE Access
Multidisciplinary | Rapid Review | Open Access Journal

Received January 15, 2021, accepted January 17, 2021, date of publication January 22, 2021, date of current version February 2, 2021.

Digital Object Identifier 10.1109/ACCESS.2021.3053100

Electromagnetic Metamaterials: A New Paradigm of Antenna Design

PRAVEEN KUMAR[1], TANWEER ALI[1], (Senior Member, IEEE), AND M. M. MANOHARA PAI[2], (Senior Member, IEEE)

[1]Department of Electronics and Communication, Manipal Institute of Technology, Manipal Academy of Higher Education, Manipal 576104, India
[2]Department of Information and Communication Technology, Manipal Institute of Technology, Manipal Academy of Higher Education, Manipal 576104, India

Corresponding author: M. M. Manohara Pai (mmm.pai@manipal.edu)

ABSTRACT The progress of technology in consumer electronics demand an antenna having a compact size, high gain and bandwidth, and multiple antennas at transmitter and receiver to enhance the channel capacity. Over the last decade, numerous techniques are proposed to improve the performance of the antenna. One such technique is the use of metamaterials (MTMs) in antenna design. MTMs are artificial structures to provide unique electromagnetic properties that are not available in natural materials. The unique properties of these materials allow the design of high-performance antennas, filters, and microwave devices which cannot be obtained using traditional antennas. Loading antenna with the one, two, and three-dimensional MTM structures comprised of a periodic subwavelength unit cell exhibits RLC resonant structures and allows to manipulate electromagnetic waves in the antenna system. These structures offer low resonant frequency compared to the antenna resonant frequency resulting in antenna miniaturization and manipulation of electromagnetic waves helps in enhancing the gain and bandwidth, and achieving circular polarization (CP) of an antenna system. Also, metamaterial loading enhances isolation between the antenna elements in the multiple-input-multiple output (MIMO) system by suppressing the surface waves. In this paper, the electromagnetics of MTM with analytical expressions and its application in antenna design are discussed in detail. The MTM-based antennas are classified into MTM loading, MTM inspired antenna, metasurface loading, and composite right/left hand (CRLH) based antennas. The recent development in MTM inspired antenna and its application in antenna miniaturization, enhancing gain and bandwidth, achieving CP and mutual coupling suppression in MIMO antenna systems are discussed to make it useful for further research.

INDEX TERMS Circular Polarization (CP), Metamaterial (MTM), gain, bandwidth, high impedance surface (HIS), mutual coupling, antenna miniaturization, composite right/left hand (CRLH).

I. INTRODUCTION

Currently, the progress of the communication system has conveyed voluminous challenges to wireless systems, particularly in the field of an antenna. The substantial role of design and development of antenna must be considered cautiously and comprehensively as the antenna is a key element in the wireless communication system and any application associated with radio engineering. The present-day telecommunication system introduces various operating frequency ranges and numerous wireless standards on a single stage. Therefore, multiband antennas are fascinating in mobile technologies stretching from 2G to 5G and comprising of IEEE 802.11 standards. On the other hand, advancement in long term evolution (LTE) imposes lower frequency operating ranges. Hence it stimulates a novel antenna design operating over a large bandwidth and it can be integrated to any handheld devices within the assigned dimensions. The development of these antennas utilizes different strategies and procedures to achieve novel structures, some of which are concisely described.

Generally, microstrip antennas are used because their TM01 and TM10 orthogonal modes offer port isolation and reduce cross-polarization [1]–[4]. To enhance bandwidth, high gain, better radiation pattern, dipole antenna comprised of electric and magnetic poles are used [5]–[7]. Multiple PCB layers are used to extend bandwidth for multiband operation by exciting resonant modes on the plates [8], [9].

The associate editor coordinating the review of this manuscript and approving it for publication was Qi Luo.

Inserting parasitic elements and various coupling techniques to the antenna improves antenna parameters such as radiation pattern, bandwidth, and isolation [10]–[14]. Resonant cavity antennas are used for enhancing antenna directivity, front to back ratio, and gain [15]. Quite recently, the metamaterial (MTM) inspired antenna has gained substantial attention from antenna researchers.

The initiation of MTM has significantly shown new design methodologies of materials, particularly materials having unusual properties when compared to available materials in nature as shown in Figure 1 [16]. One of the significant classes of MTMs is electromagnetic MTMs (commonly mentioned as an MTM), which are engineered sub-wavelength structures. Generally, MTMs are defined as engineered artificial materials comprising of periodic or non-periodic structures of unit cells with its diameter less than the wavelength of light being propagated through it [17]. Such an artificially implemented array of unit cells can create an electromagnetic response that can be customized evenhandedly by magnetic and electric wave components. Therefore, a periodic array of unit cells can be considered as an efficient material described by its permittivity and permeability parameters. This arrangement agrees to constitute electromagnetic responses at the required frequency, such response will not exhibit in material presents in nature. For instance, magnetic materials are much bounded at microwave frequencies. However, array periodic structures of metallic rings demonstrate such magnetic response at high frequencies.

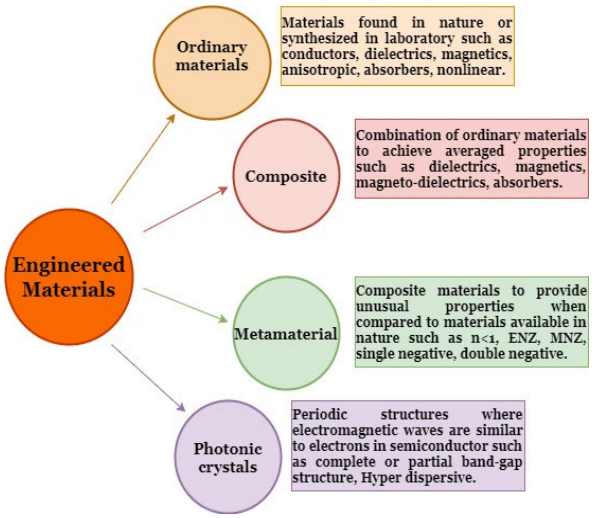

FIGURE 1. Classification engineered material based on electromagnetic properties [16].

Rotman demonstrated negative effective permittivity by assembling an array of metal wires [18]. In 1968, Veselago [19] theoretically shown the material having simultaneous negative values of permittivity and permeability disclosing a phase velocity as negative. The electromagnetic response of an array of metal wires and rings are shown by Pendry [20], [21]. Later based on this work Smith [22], [23] established a medium experimentally to confirm simultaneous effective permittivity and permeability to be negative.

In this paper, we provide an exhaustive review of metamaterials used for performance improvement in various antenna designs utilized for wireless communication. The main contributions of this paper are as follows,

- Detailed analysis of metamaterial properties and also the effect of geometrical properties on SRR are discussed.
- The influence of metamaterial in antenna design to obtain miniaturization, gain and bandwidth enhancement, and realizing circular polarization are also described.
- Additionally, the significance of metamaterials on mutual coupling suppression/isolation enhancement in the MIMO antenna system is described.

This paper is organized as follows: In section II classification of materials, conditions for accomplishing negative permittivity and permeability are discussed. Section III presents the impact of MTM on antenna miniaturization. Section IV discusses the influence of MTM in enhancing the gain and bandwidth of the antenna. Section V describes the impact of MTM to achieve the circular polarization antenna. Mutual coupling suppression in MIMO antenna systems using metamaterials is presented in Section VI. Finally, concluding remarks and future directions are given in Section VII.

II. CLASSIFICATION OF MATERIALS

One way of classification of natural and MTM is based on the propagation phase constant (β) of the current flowing through the antenna element [24]. The material is classified as natural if the value of β is greater than zero ($\beta > 0$). For example, Figure 2a illustrates the antenna where the flow of current from feed point F has phase constant positive ($\beta > 0$). The phase distribution in such antenna receipts a regressive form, resulting in a lag of phase from point F to antenna ends. The material is classified as MTM if the value of β is less than zero ($\beta < 0$) for a particular frequency band or zero at the non-zero frequency ($\beta = 0$). For example, Figure 2b illustrates the β of the outgoing current is negative ($\beta < 0$) within a particular band of frequency or zero at the frequency of non-zero ($\beta = 0$). The phase distribution in such antenna receipts a progressive form from point F to antenna ends and $\beta = 0$ indicates infinite long wavelength. This kind of antenna is classified into an MTM antenna or MTM-based antenna.

A. MTM

The electric permittivity (ε) and magnetic permeability (μ) are used to characterize an electromagnetic material as shown in Table 1 and Figure 3 [17], [24]–[26]. The right-handed (RH) material having $\varepsilon > 0$ and $\mu > 0$ demonstrates the phase constant of wave propagation (β) to be a positive value ($\beta > 0$) and is termed as double-positive (DPS) material. The single negative material such as epsilon negative (ENG) having $\varepsilon < 0$ and $\mu > 0$, and mu negative (MNG) having

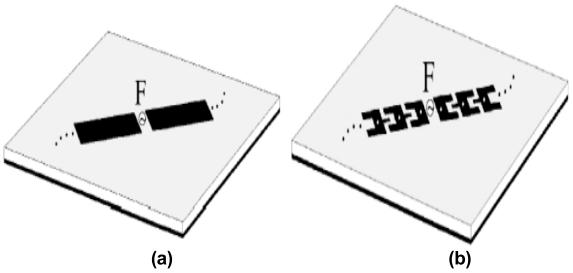

FIGURE 2. Antenna classification (a) Natural antenna (b) MTM antenna [24].

$\varepsilon > 0$ and $\mu < 0$) exhibits phase constant of wave propagation is zero ($\beta = 0$, evanescent). The left-handed (LH) material having $\varepsilon < 0$ and $\mu < 0$ demonstrates the phase constant of wave propagation to be a negative value ($\beta < 0$) and is termed as double negative (DNG) material. An RH material is easily found in nature, whereas ENG, MNG, DNG materials are artificial and referred to as MTM.

TABLE 1. Special material properties in ε-μ domain.

Permittivity (ε)	Permeability (μ)	Description
$\varepsilon = -\varepsilon_0$	$\mu = -\mu_0$	Characterizes anti-air in left-hand medium, yields to the perfect lens.
$\varepsilon = 0$	$\mu = 0$	Characterizes a nihility, yields to the perfect tunneling effect.
$\varepsilon > \varepsilon_0$	$\mu = \mu_0$	Characterizes the material available in nature.
$\varepsilon = \mu$		Characterizes perfect impedance matching in right-hand medium and left-hand medium, ensuing no reflections.

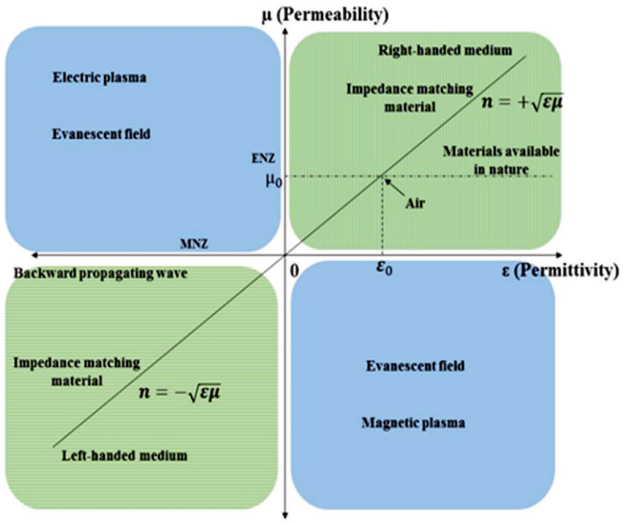

FIGURE 3. Material classification is based on permittivity and permeability.

B. NEGATIVE PERMITTIVITY MATERIAL

The ε negative materials are the materials having ε negative and μ positive and represent electric plasma. To stimulate surface Plasmons, it is necessary to have roughness in the surface, a dielectric coupler to vacuum like hemisphere or prism, and a metallic strip structure [27], [28].

An array of thin metallic wires are organized periodically in a dielectric medium or vacuum to exhibit low-frequency stopband characteristics from zero to a certain cut-off frequency. Rotman [18] systematically investigated various arrangements of 1D, 2D, and a 3D array of wire network structures to induce resonance in the polarized electric field at lower than the plasma frequency. Such an artificial composite wire structure creates a negative electric permittivity with manageable strength. The effective permittivity of an array of wire in Drude form can be written as in equation (1).

$$\varepsilon_{eff}(\omega) = 1 - \frac{\omega_p^2}{\omega^2 + j\frac{\varepsilon_0 a^2 \omega_p^2}{\sigma \pi r^2}} \tag{1}$$

The above equation describes dependency between the frequency of the complex permittivity and wire structure (lattice constant and radius of the wire). Several other derivations are available for finding effective plasma frequencies that are more complex but offer a precise solution are listed in Table 2.

TABLE 2. Expressions for effective plasma frequency.

Author/Reference	Effective plasma frequency
Sarychev AK, Shalaev VM [29]	$\omega_p^2 = \frac{2\pi c_0^2}{a^2\left[\ln\left(\frac{a}{\sqrt{2}r}\right) + \frac{\pi}{4} - \frac{3}{2}\right]}$
Maslovski SI, Tretyakov SA, Belov PA [30]	$\omega_p^2 = \frac{2\pi c_0^2}{a^2\left[\ln\left(\frac{a^2}{4r(a-r)}\right)\right]}$
Belov PA, Tretyakov SA, Viitanen [31]	$\omega_p^2 = \frac{2\pi c_0^2}{a^2\left[\log\frac{a}{2\pi r} + 0.5275\right]}$

C. NEGATIVE PERMEABILITY MATERIAL

The μ negative materials are the materials having μ negative and ε positive and represent magnetic plasma. The absence of magnetic response at the optical range is due to the weak coupling of the magnetic field component of light with an atom and is equal to the Bohr magneton [32]. Some of the arrangements which exhibit magnetic response at microwave and higher frequencies with negative permeability are coupled nanorods, nanoplates, and strips, an array of metallic staple, and split ring resonator (SRR). The most general structure used for achieving negative permeability is an SRR [33]–[35]. Pendry and his team established a structure comprising of two opposite facing concentric split-ring resonators at sub-wavelength dimensions as shown in Figure 4.

The gap in each metallic ring circularly prevents the development of current. The charges gather at the edge of the gap in the metal ring and exhibit capacitance behavior. Therefore,

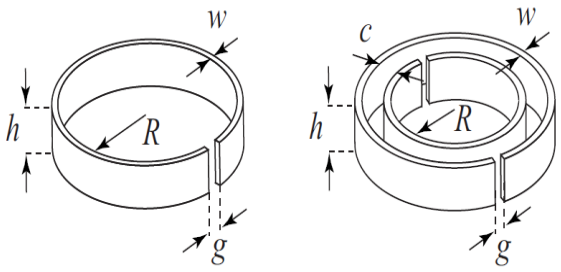

FIGURE 4. Magnetic material resonator [36]. Single ring split (left side), double ring split (right side).

the presence of an inductor and capacitor in a metal ring makes an SRR as a resonant element. The analytical expressions for determining effective inductance and capacitance are given in [36].

Several other analytical expressions are available in the literature for appropriately determining inductance, capacitance, and the resonant frequency of different resonator structure such as SRR, loop gap, and CSRR [37]–[44]. The negative permeability material structures are not just limited to circle/ring structures, but various other geometrical structures can also be used to create negative permeability such as spiral, swiss roll, square, hexagonal [45]–[52]. The transmission and reflection characteristics of the SRR depend on shape and structure. For single SRR with two varying split gaps along the ring gives rise to a change in the resonant frequency of the SRR over a wide range of frequency [53]. For double split-ring resonators, the influence of the geometrical parameters on SRR is listed in Table 3 by varying one parameter at a time and keeping other parameters constant [54]. So far numerous design structures have been available in literature in the field of MTMs. The most common ones are rectangular and circular SRR. The rectangular SRR dominates circular SRR in terms of miniaturization and dense packing [55], [56].

D. COMPOSITE RIGHT/LEFT-HANDED (CRLH) MTM

In recent years MTMs having ε/μ negative value gained substantial consideration in science and engineering communities commonly termed as left-handed material (LHM). The unique electromagnetic properties of these materials offer novel conceptualization, devices, and applications to be developed. The physical realization of these LHMs is mainly based on the transmission line and resonator method. Practically these materials exhibit left-handed material properties at a certain frequency and right-handed material properties at other frequencies, which naturally occurs. The materials which show these properties are generally termed as CRLH MTMs, introduced by Caloz [25]. Analyzing such materials with the transmission line (TL) method is referred to as CRLH-TL. One, two, and three-dimensional CRLH materials are examined by developing its equivalent TL model using inductors and capacitors as shown in Figure 5. In CRLH, right-handed TL (RHTL) is represented by a low pass configuration of a series inductor and parallel capacitors and interchanging capacitor and inductor will form a high pass configuration resulting in group and phase velocity are opposite to each other and termed as left-handed TL (LHTL).

TABLE 3. Effect of geometrical properties on SRR [56]–[58].

Geometrical parameters	Effect on SRR
Increasing the split-gap of SRR	As the split gap increases, the value of the capacitance decreases leads to a decrease in total capacitance, and a decrease in capacitance value increases the resonant frequency.
Increase in spacing between two adjacent rings of SRR	The increase in spacing between the rings reduces the mutual inductance and capacitance, respectively. Due to a decrease in inductance and capacitance resonant frequency increases as analytically expressed in [59].
Increasing the side length of SRR	Increasing the side length of SRR increases the effective value of inductance and thereby shifts cutoff frequency towards the lower frequency.
Increase in metal width	The increase in metal width reduces mutual inductance and mutual capacitor and thereby increases the resonant frequency.
Multiple split gaps in SRR	Multiple gaps in SRR intercept magnetic resonance because of the induced current by an electric field and shift resonant frequency towards the higher frequency [58].

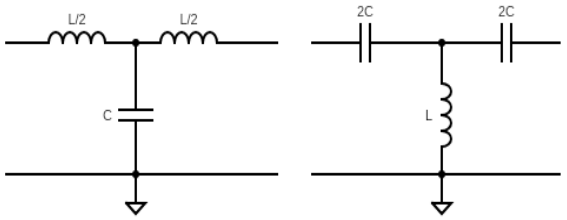

FIGURE 5. Right-handed transmission line (left), Left-handed transmission line (right).

The equivalent LC networks are realized by generating the required physical inductors and capacitors [60].

Generally, these LC networks are analyzed by either surface mount technology (SMT) chip components or distributed components based on the requirements of the application. SMT-based CRLHs are confined to low frequencies and it is complex to implement in radiating applications. The distributed component based CRLHs are implemented by a coplanar waveguide (CPW), stripline, microstrip line, and so on.

III. IMPACT OF MTM IN ANTENNA MINIATURIZATION

In this section, the influence of MTM in antenna design for miniaturization is discussed. The ever increasing demand for electronic gadgets and wireless connectivity to the internet of things (IoT) urges for antenna miniaturization. The term antenna miniaturization refers to reducing the size of an antenna while maintaining acceptable performance when

compared to the original antenna. Over the last decade capacity to reduce the physical size of an antenna without comprising performance degradation has been of great interest in the field of antenna design [61]. In the literature, numerous approaches are proposed for antenna miniaturization such as using high permittivity and permeability material, modification antenna structures, loading resistors, capacitor, and inductor components [62]–[67]. The present-day numerous MTM based techniques are evolved for reducing the size of different antennas such as integrated antennas, patches, dipoles, loops, slots, and leaky-wave, etc. [68], [69]. Figure 6 illustrates different MTM based approaches for antenna miniaturization such as MTM loading, MTM inspired, metasurface loading, and CRLH based antennas [61], [70].

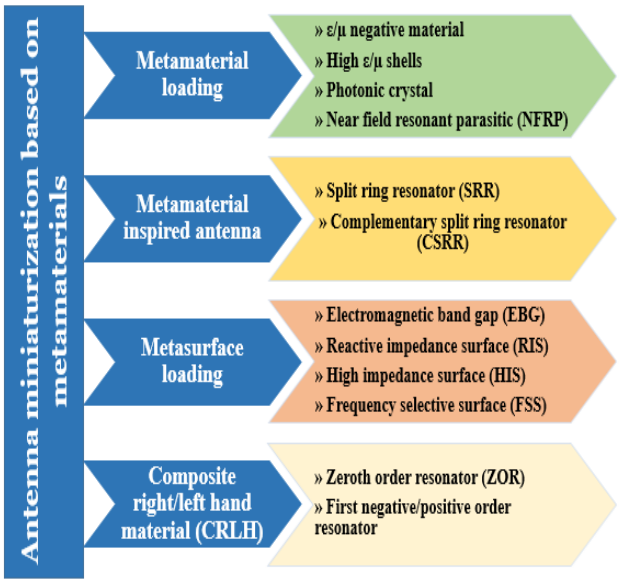

FIGURE 6. Miniaturization of antenna based on MTMs.

A. MTM LOADING

The design challenges associated with the electrically small antennas (ESA) are achieving proper resonating conditions, compact size, etc. [71]. As the size of the antenna reduces operating wavelength shrinks and therefore it is difficult to maintain impedance matching. To overcome these challenges one method is loading antenna with MTM structures comprised of periodic subwavelength unit cells.

The MTM loading antenna refers to antennas whose properties are because of interaction between effective MTM medium and antenna. This type of antennas offers compact size, high gain, and bandwidth, etc., and is advantageous when compared to the traditional antennas. Different techniques of MTM loadings are ε/μ negative materials, high ε/μ shells, photonic crystals, near field resonators, and so on [72]–[77] as shown in Figure 6. The ε negative based MTM loading is analyzed using a transmission line (TL). ENG TL offers negative permittivity at a lower frequency, positive permittivity at a higher frequency, and zero at a particular frequency. The resonance mode of the ENG TL is given by equation (2).

$$\theta = \beta l = \beta N p = n\pi, \quad n = 0, 1, \ldots, (N-1) \tag{2}$$

where N is the number of unit cells. For the frequencies associated with resonant length $\theta = \beta l$ of a TL resonator, the resonance frequencies are multiples of π. The phase constant of ENG TL is expressed using periodic boundary conditions as in equation (3) [78].

$$\beta p = \cos^{-1}\left\{1 - 0.5\left(\frac{\omega^2 - \omega_E^2}{\omega_R^2}\right)\right\} \tag{3}$$

where p is the unit cell length, 0^{th} and 1^{st} order frequencies of ENG TL is defined in equation (4).

$$\omega_E = \frac{1}{\sqrt{L_L C_R}} \quad and \ \omega_R = \frac{1}{\sqrt{L_R C_R}} \tag{4.a}$$

$$\left.\begin{aligned} \omega_0 &= \omega_E = \frac{1}{\sqrt{L_R C_R}} \\ \omega_1 &= \sqrt{2\omega_R^2 + \omega_E^2} = \sqrt{\frac{2}{L_R C_R} + \frac{1}{L_L C_R}} \end{aligned}\right\} \tag{4.b}$$

The antenna based on zeroth-order (ZOR) resonator provides infinite wavelength at frequencies other than zero with zero phase constant [79]. This feature makes it independent of the physical dimension of the antenna. As mentioned in equation (4), it depends on the values of the inductor and capacitor. Therefore, ZOR is an excellent technique to miniaturize an antenna as it does not depend on the physical dimensions of an antenna rather it requires tuning of distributed lumped elements [80]. The ZOR is formed either by using ENG TL/mu negative TL or composite right/left-handed (medium) TL [81]. In [74] a wire monopole antenna is miniaturized from 29.5mm to 16 mm using an array of a single ring SRR as MTM loading. This single ring SRR arrangement increases the reactance (inductive) and permeability of the effective medium and helps to form a high refractive index medium. Thus, increases in the refractive index of effective medium reduce the length of the monopole antenna with the same fundamental resonance frequency of 2.5 GHz compared to the unloaded original antenna without degradation in antenna performance as shown in Figure 7 (b).

B. MTM INSPIRED ANTENNA

Antenna miniaturization is due to the placing of metaresonators into the antenna structures. In this approach, the properties of an antenna are due to single or more than two-unit cells interact with the antenna structures. When such unit cells are arranged in an array configuration, structures exhibit unique characteristics such as ENG, mu negative (MNG), and double-negative (DNG) [82]–[87]. These unique characteristics are because material behaves as resonant structures. The resonating frequency of these structures is less than the resonant frequency of the antenna as discussed in section 2. MTM inspired antenna can be achieved by engraving the unit cell structures into the radiating patch or ground plane or

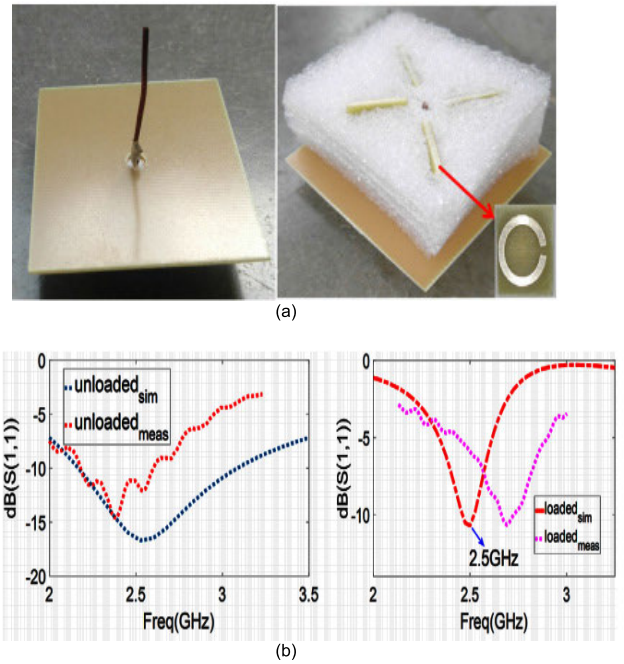

FIGURE 7. Quarter wavelength monopole antenna (left) and miniaturized monopole antenna loaded with high refractive index [74] (a) Antenna design (b) Return loss.

between the ground and radiating plane. This approach is very similar to introducing a slit/slot into the antenna structure, but this unit cell arrangement acts as a resonant structure. As an example, in [83], a quad-band antenna consisting of a double-printed hexagonal slotted radiating patch with rectangular SRR is proposed for miniaturization and reported 16.7% and 33.94% size reduction concerning active patch area and volume with acceptable gain, good radiation characteristics, and impedance matching as shown in Figure 8.

C. METASURFACE LOADING

Metasurfaces are artificial thin layers consisting of uniform or non-uniform periodic elements with subwavelength/deep subwavelength dimensions. Different types of metasurfaces are high impedance surface, reactive impedance surface, frequency selective surface, and electromagnetic bandgap as shown in Figure 6. High impedance surfaces (HIS) are a periodic organization of metallic shapes of sub-wavelength size on dielectric material with metal ground plane on another side [88]. HIS is an engineered arrangement that shows a low reflection phase (θ) over some frequency range and at some other frequency range, it suppresses all surface waves. HIS structures are analyzed by their equivalent LC circuit configuration. The reflection phase for incident wave normal to the surface is given by equation (5) [89].

$$\theta = Im\left[\ln\left(\frac{Z_{HIS}-\eta}{Z_{HIS}+\eta}\right)\right] \tag{5}$$

where Z_{HIS} is the surface impedance and Z_{HIS} is low, $\theta = \pm\pi$, Z_{HIS} is very high, $\theta = 0$ and impedance of surface is equal to the impedance of free space then phase reflection

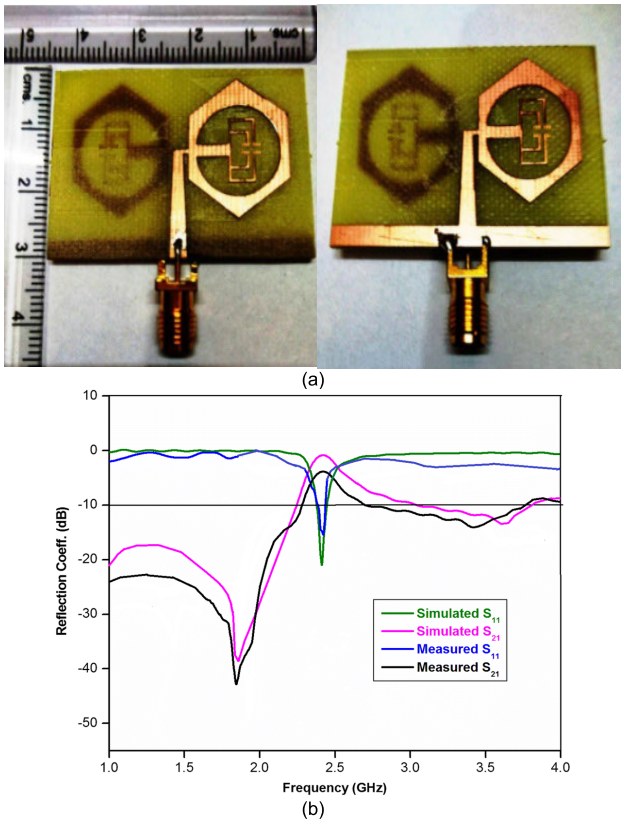

FIGURE 8. Miniaturized antenna using MTM loading index [83] (a) Antenna design (b) reflection coefficient.

crosses$\pm\frac{\pi}{2}$, η is the impedance of the medium. When the phase reflection is zero then the surface acts as an artificial magnetic conductor (AMC). It means that the radiated fields of the image current add positively when the source is placed horizontally at a distance $h < \lambda_0/4$. This configuration doubles the fields and at the same time reduces antenna thickness by acting as artificial ground. The reactive impedance surface (RIS) is a sub-wavelength periodic arrangement of shapes, which has the capacity of magnetic/electric energy storing and reflects power like a perfect magnetic conductor (PMC) or perfect electric conductor (PEC) surfaces [90]. The RIS structures loaded with antenna reduces the size by providing high propagation constant resulting in a shorter wavelength at the desired frequency. However high propagation constant leads to poor impedance matching. In this scenario, the feed point of an antenna plays important role in impedance matching. In [91] patch antenna miniaturization is reported using RIS as shown in Figure 9. The RIS substrate makes an antenna to resonant at a lower frequency because of its reactance, inductance, and capacitance characteristics and resulting in a small volume compared to the original planar antenna dimensions with acceptable efficiency. Even RIS enhances antenna efficiency and impedance matching by reducing contact between antenna and substrate [92]. The frequency selective surfaces (FSS) are also one, two, two and half, three-dimensional periodic structures exhibiting band pass or band stop characteristics. Over the last few years,

different FSS structures are proposed for miniaturization such as substrate integrated waveguide, lumped element loading, loops, patches, multi holes, and so on [93]–[96]. The two-element patch antenna array is proposed in [97] using an electromagnetic bandgap ground plane. The array antennas are miniaturized using periodic EBG structure as ground plane by replacing conventional metal ground plane as it reduces the distance between the unit cells. It also enhances isolation in array antennas.

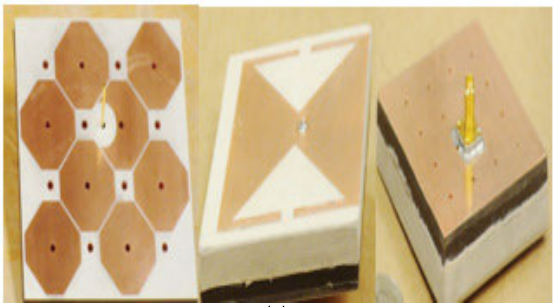

(a)

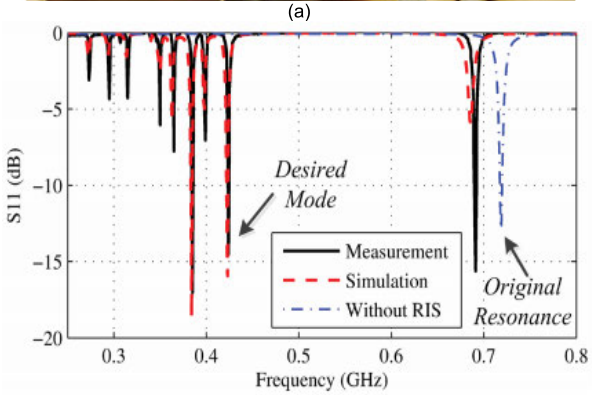

(b)

FIGURE 9. Antenna miniaturization using RIS. A 4 × 4 unit cell RIS (left), the front side of patch antenna mounted on 4 × 4 unit cell RIS (center), and backside of patch antenna (right) [91] (a) Antenna design (b) Return loss.

D. CRLH/RESONANT DISPERSION

The utilization of MTMs in antenna and microwave devices for miniaturization is shown in [25], [98]. A composite right and left-handed MTM give a theoretical analysis for designing compact antennas. In [99] developed a miniaturized microstrip patch antenna based on the fractal shape of right-handed material and a left-handed material-based unit cell is loaded nearby the antenna for miniaturization as shown in Figure 10. The loaded MTM unit cell acts as a parasitic load and alters the inductance value thereby antenna size is reduced by 24%. A miniaturized ultrawideband antenna with an improved gain is developed based on the CRLH unit cell in [100]. The CRLH unit cell is constructed using an I-shaped slot on the patch forms capacitance and a thin microstrip line in spiral shape is grounded by metal thru a hole that forms an inductor. The antenna is miniaturized using properly tuned capacitance value by adjusting the gap between I-shaped slots.

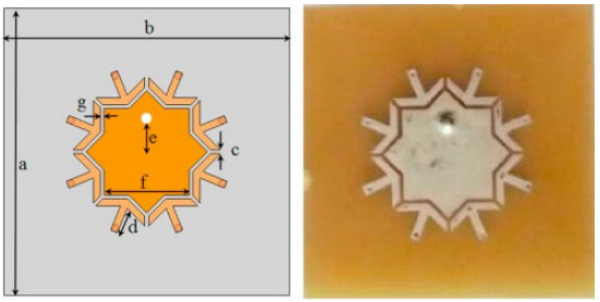

(a)

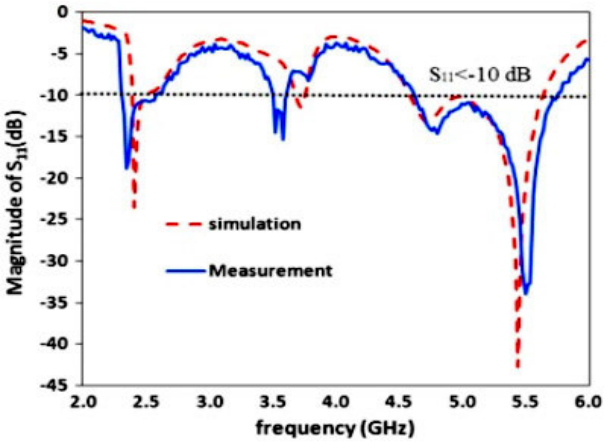

(b)

FIGURE 10. Schematic and miniaturized patch antenna based on CRLH [99] (a) Antenna design (b) magnitude of S_{11}.

E. SUMMARY

The advancements of technology in consumer electronics demand a miniaturized antenna without performance degradation. The literature reports a different methodology for antenna miniaturization. The availability of MTM attracted antenna design researchers in recent years due to its unique characteristics, which are not available in the material available in nature. Loading antenna with MTM structure based on MNG, ENG, DNG, high epsilon/mu, a combination of high and low dielectric material, and near filed parasitic elements, ultimately exhibits RLC based resonant structures. The SRR and CSRR unit cells also exhibit resonant structures. When these unit cells are placed nearby, an antenna shifts the resonant frequency to the lower side. The stimulus of these unit cells is due to the excitation of electromagnetic waves by an antenna.

The unit cell induces a resonant frequency that is less than the resonant frequency of the antenna resulting in the preferred miniaturization of the antenna. The periodic arrangement of metallic patches or apertures leads to different metasurfaces such as reactive impedance surface, high impedance surface, or electromagnetic bandgap structure, and FSS loading with the antenna leads to miniaturization of an antenna with improved performance. By forming an in-phase current in the antenna using CRLH unit cell loading allows reducing the size of the antenna. The aforementioned different techniques of antenna miniaturization using

TABLE 4. Influence of MTM in antenna miniaturization.

Ref	MTM technique	f, GHz	Max gain, dBi	Max efficiency, %	S_{11} bandwidth, %	Size reduction, %	Dimension, λ_0
[71]	ENG-TL	2.66	3.42	86.2	21.5	-	0.213×0.237×0.012
[101]	Complimentary capacitvely loaded loop	3	4	>95	8.1	79.5	0.15×0.09×0.007
[65]	Meandered PIFA on magneto dielectric nano composite surface	0.946	1.26	74.19	7.24	-	0.075×0.075×0.003
[80]	ENG-TL complementary concentric closed ring resonator	1.16, 2.32, 3.58	1.59, 2.1, 4.97	73, 82, 95	8.54, 10.25, 35.75	-	0.11×0.11×0.006
[102]	CSRR and MTM slab	2.34	-0.6	84.2	5.3	56.7	0.23×0.23×0.009
[103]	Elliptical shaped SRR	2.78, 6.02	-	83.33, 99.38	3.59, 25.41	-	0.259×0.203×0.014
[85]	CSRR	1.8	7	-	-	48	0.97×0.73×0.009
[87]	CSRR	7.5	4.7	82	120	-	0.23×0.29×0.015
[74]	High refractive index	2.5	-1.4	-	-	45.7	0.41×0.41×0.13
[95]	FSS	1.59, 1.96	-	-	-	-	0.042×0.042×0.0007
[92]	RIS and partially reflective surface	5.85	12.5	-	24.3	-	1.55×1.55×0.11
[79]	ZOR	3.7	1.59	91.5	25.4	57.9	0.095×0.042×0.013
[104]	SRR and CRLH-TL	3.30	5.4	74	14.1	-	0.277×0.277×0.033
[73]	CRLH, SRR	1.62, 2.78	1.05, 2.59	98.5, 97.2	2.46, 1.07	51.9	0.162×0.108×0.008

- Not available

metamaterial is summarized in Table 4 with the antenna dimension in λ_0 and antenna performance such as gain, efficiency, and bandwidth.

IV. IMPACT OF MTM ON GAIN AND BANDWIDTH ENHANCEMENT

In wireless communication apart from antenna miniaturization the need for wide bandwidth and high gain is increasing in recent years. At the same time, compact low profile antennas suffer from performance degradation in gain and efficiency due to poor radiation characteristics [105]–[108]. The literature presents numerous approaches to increase the gain and bandwidth of an antenna such as introducing vias, parasitic elements, modifying ground planes, and so on [109]–[113]. Although these techniques improve radiation characteristics but at the cost of increased complexity. In this regard introducing MTM with a distinct resonator structure have a great impact on minimizing complexity and improving antenna parameters.

A. MTM LOADING

The different MTM structures loading in association with the antenna improve gain and bandwidth of the antenna. The different structures of MTM will provide different resonating frequencies. An ultrawideband is presented in [114] uses a planar MTM structure as shown in Figure 11. The proposed antenna is developed on a flame retardant (FR)-4 substrate of size 32 mm×28mm with a mesh shaped radiating element and the ground plane defected by a cross shape of size 2 mm×2 mm. This modification of the ground plane offers more discontinuity and hence antenna structure stores less energy and radiates more energy, resulting in peak and an average gain of 8.02 dB and 4.5 dB, the impedance bandwidth of 3.06 - 36.4 GHz (Two-fold bandwidth of ranges 3.08 - 11.7 GHz and 13.6 - 36.4 GHz).

In [115] a conventional microstrip antenna is developed on an FR4 substrate of size 15 mm × 10 mm with a thickness of 1.5mm. The proposed antenna utilizes a double negative (DNG) MTM lens layer to improve the gain of 71% (i.e. 4.36 to 7.45 dB) as shown in Figure 12. The increase in gain is because of placing the antenna and lens at an appropriate distance. In this case distance between the antenna and the first lens is 10 mm and between the two lenses is 5 mm. A DNG MTM unit cell delivers a natural impedance matching network and it increases the radiated power and correspondingly decreases reactance of the structure so that

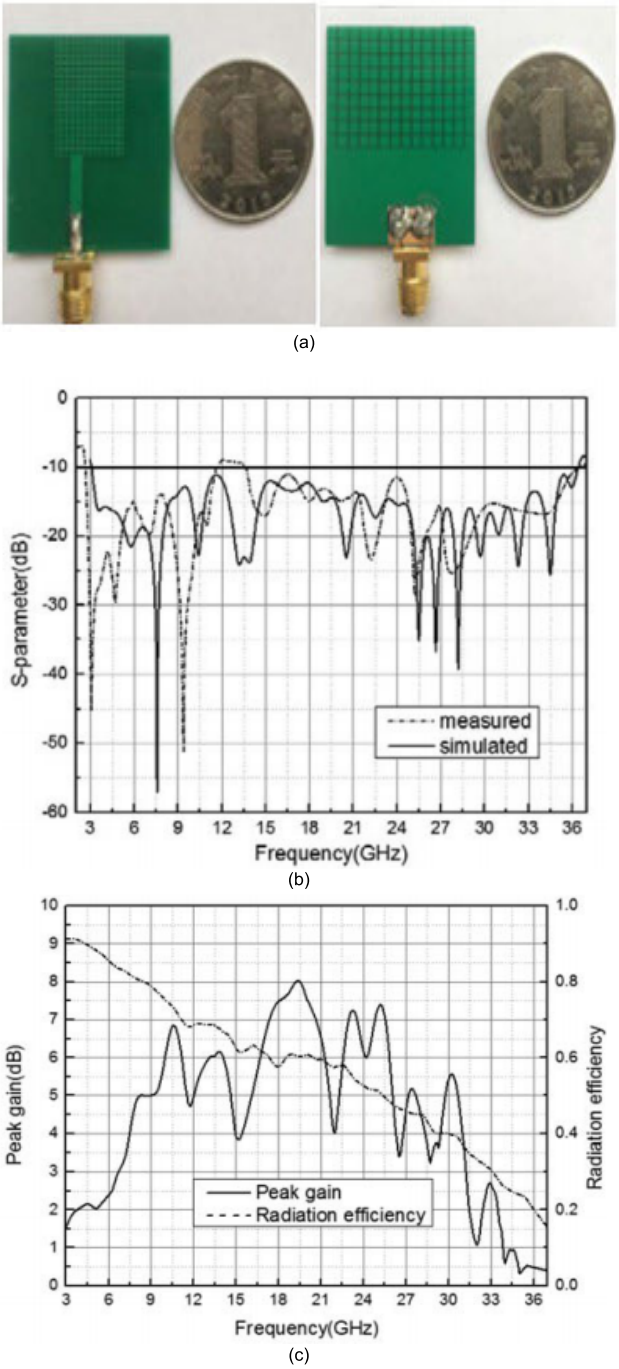

FIGURE 11. Microstrip antenna based on MTM to increase gain and bandwidth [114] (a) Antenna design (b) S-parameter and (c) peak gain and radiation efficiency.

the gain of antenna increases [116]. The right arrangement of high permittivity material above or below the low permittivity material results in wider bandwidth up to 20% or even higher. Even high gain can also be achieved by properly selecting high permittivity material and physical dimension ratio (i.e., height to length ratio).

In [117] a dielectric resonator antenna is proposed based on high permittivity material for improving gain and bandwidth of the antenna. It is reported that the proposed antenna has

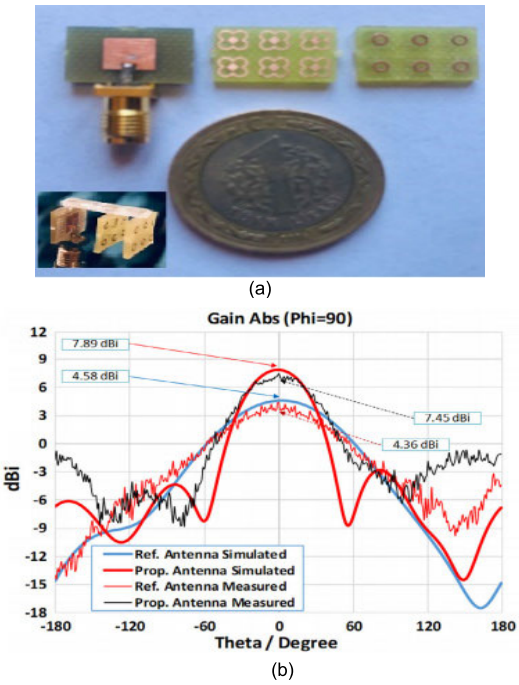

FIGURE 12. Microstrip antenna with a lens of DNG MTM to increase gain [115] (a) Antenna design (b) Absolute gain.

an impedance bandwidth of 40% (3.97 to 5.98 GHz) and an average gain of 10.2 dBi as shown in Figure 13. The amplitude and propagation direction of electromagnetic waves is controlled by leaky waves. The important property of metasurface allows manipulating surface wave leakage that results in improving the performance of the antenna [118]. In [119] designed a microstrip antenna based on the photonic crystal on the FR4 substrate having a gain of 5.93 dB, directivity of 6.92 dB, and maximum fraction bandwidth of 7.86%. The proposed antenna uses periodic and nonperiodic structures to develop a photonic bandgap, which eliminates surface waves and by lowering the rear and side lobes improves the performance of the antenna.

Apart from many techniques to enhance the gain and bandwidth of an antenna, near field resonator parasitic (NFRP) is a potential solution to overcome the hindrance of compact planar antennas. The NFRP elements together with the antenna have many advantages such as high radiation efficiency, good matching network without any external circuit, and easy fabrication. There are numerous methods adopted to enhance antenna parameters using NFRP. They are broadly classified into passive and active NFRPs [120]–[122]. NFRP based antenna is proposed in [123] has demonstrated 14.4% impedance bandwidth and 1.4 dBi realized gain over the operating frequency. The enhancement of frequency is because of an increase in capacitance value due to the center gap and between the patches as shown in Figure 14. The increase in capacitance influences the patches to operate 180 degrees out of phase at the second dipole mode resulting in a wider bandwidth and stable radiation properties.

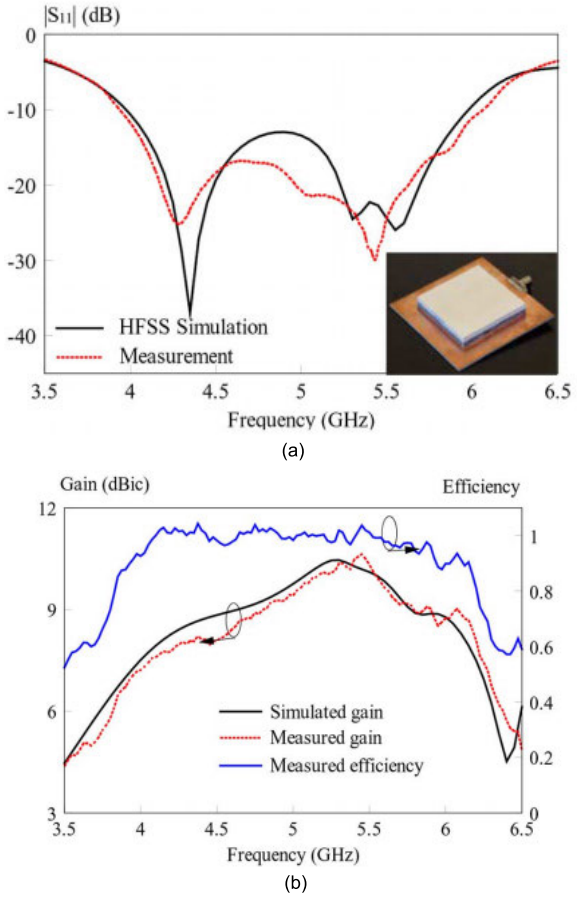

FIGURE 13. A dielectric resonator antenna with high permittivity to increase gain and bandwidth [117] (a) Return loss (b) Gain and efficiency.

B. MTM INSPIRED ANTENNA

The subwavelength structures exhibit negative permittivity and permeability, the reversal of Doppler's effect, and Snell's law. Because of this nature, these electromagnetic MTM is used to enhance the performance of the planar antenna. The most common structures are split-ring resonator and complementary split-ring resonator, and a combination of strips with SSR and CSRR as discussed in the aforementioned section. In [124] a CSRR is used to improve the gain of the microstrip antenna as shown in Figure 15. By introducing CSRR on the ground plane of the patch exhibit a good gain of 5.93 dBi at a resonant frequency, slightly more bandwidth, and also reduction of size by 10% compared to the unloaded antenna. SRR structures are used to enhance the bandwidth of the microstrip antenna by stimulating and combining two resonant modes as shown in Figure 16 [125]. In [126] a microstrip antenna is proposed using corrugated and non-corrugated SRR to enhance gain and bandwidth of the antenna. The proposed antenna improves bandwidth from 230 to 420 MHz and the gain from 6.2 to 7 dB.

The crossed SRRs stimulated dual capacitor ring resonator (DRR) and crossed DRR is proposed in [127] for realizing high gain as well as miniaturization of an antenna. The circularly polarized antenna is configured on an F4BM substrate

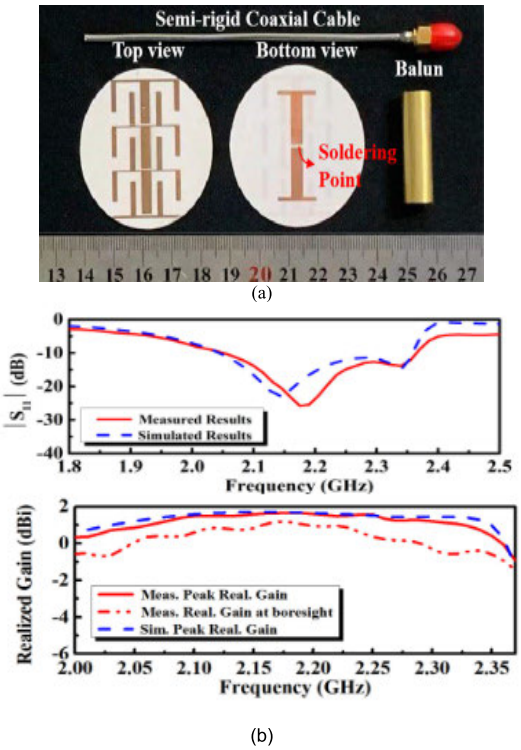

FIGURE 14. A dipole antenna based on NFRP and its radiation performance [123] (a) Antenna design (b) Return loss and realized gain.

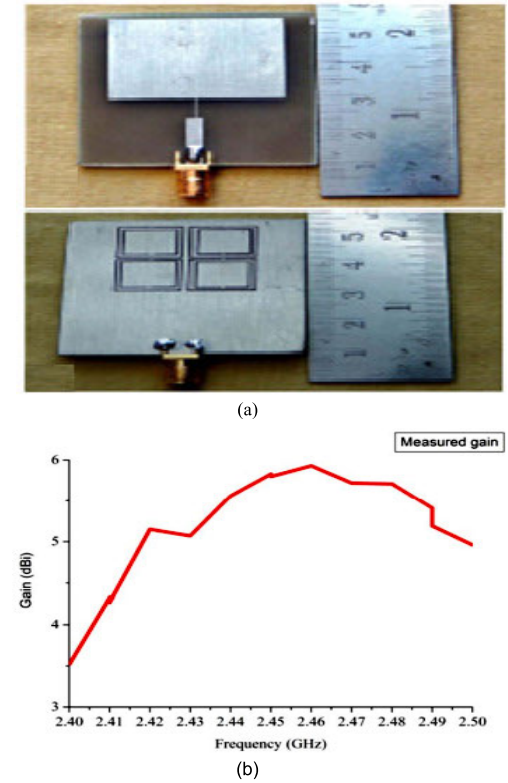

FIGURE 15. Antenna loaded with CSRR for gain enhancement [124] (a) Antenna design (b) Measured gain.

with copper layers on both sides of the substrate with a thickness of 0.018mm. An aluminum sheet having a thickness of 0.8mm is used to form a ground layer. Metallic screws

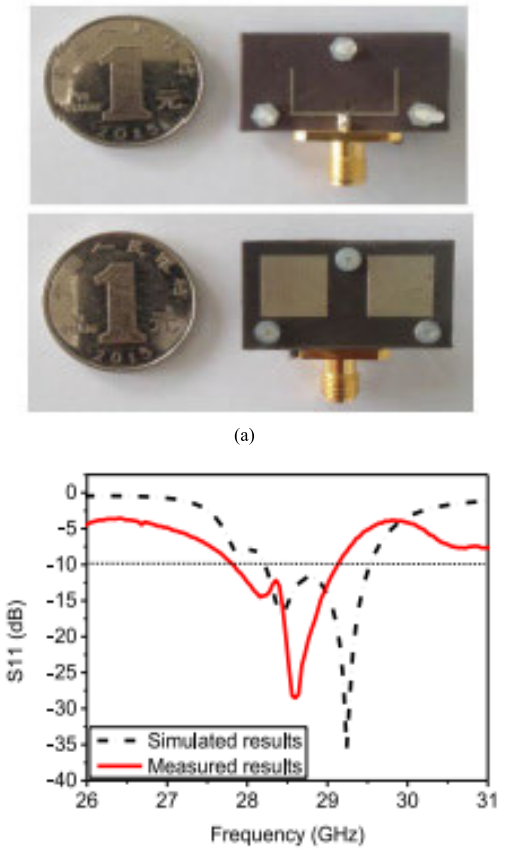

FIGURE 16. Antenna loaded with SRR for bandwidth enhancement [125] (a) Antenna design (b) Return loss.

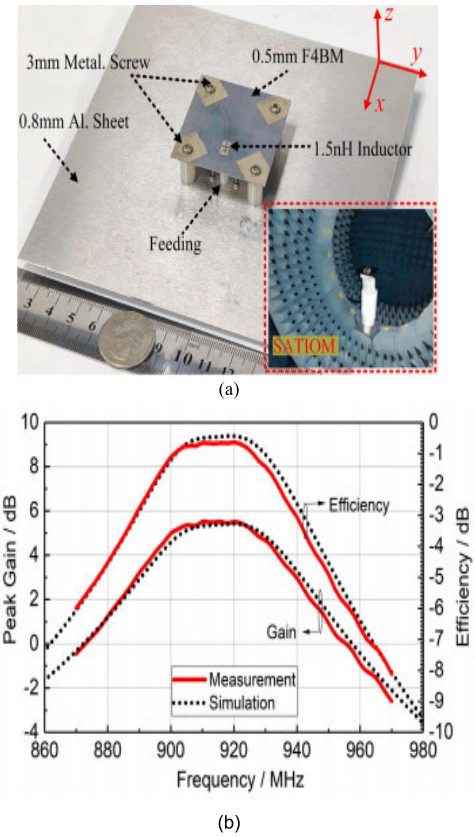

FIGURE 17. Circularly polarized antenna with cross-shaped SRRs and it's gain and efficiency [127] (a) Antenna design (B) peak gain and efficiency.

are used to support substrate with the ground plane as shown in Figure 17. A metal-insulator-metal capacitor is formed by an overlying dielectric substrate between two copper conductors. Metallic screws deliver total inductance in the structure. The arrangement has air in-between substrate and ground plane to reduce dielectric loss and is expected to achieve good radiation efficiency. For stimulating the antenna coaxial feed line is used and to optimize the matching inductor, capacitor, and feed point is fine-tuned for RFID applications.

C. METASURFACE LOADING

Low profile antennas commonly suffer from narrow bandwidth and low gain. There are multiple approaches reported in the literature to enhance the gain and bandwidth of an antenna including metasurface loading recently. The rich environment of manipulating electromagnetic waves in metasurface incorporating with patch antenna improves gain and bandwidth.

The development of antenna using metasurface involves an arrangement of meta-atoms having a size of subwavelength and separated by subwavelength distance from one another. In this type of antenna, metasurface behaves as an antenna aperture and radiates or receives electromagnetic waves from or into the feed line of the antenna. The advantages of metasurface in antenna design are gain and bandwidth enhancement, suppression of mutual coupling, low RCS, frequency scanning, etc. The patch antenna developed in [128] using non-uniform patches of the metasurface, stair shaped aperture, and coplanar waveguide feeding with a peak gain of 9.18 dBi and impedance bandwidth of 67.3% as shown in Figure 18. Every subwavelength patch behaves as a radiating element and altogether it acts as an array of a radiating plane and improves the gain of an antenna. The bandwidth of a proposed antenna is improved by increasing coupling between metasurface and stair shaped aperture placed at the top and bottom of the substrate.

In [129] Fabry-Perot cavity antenna is proposed for gain and bandwidth improvement. The partially reflective surface is designed by printing a ring on the upper side of the superstrate and an etched circular ring on the bottom side as shown in Figure 19. By optimizing the physical dimensions of circular rings on both sides of the superstrate a positive phase gradient is achieved. The realized positive gradient of the PRS array demonstrates an improved gain of 11.2 dB. A pair of slot stubs are inserted on the rectangle slot where the current is zero to form a feeding line for the slot antenna. This configuration gives an impedance bandwidth of 22.2% (14.8-18.5 GHz) and two resonant modes.

Electromagnetic bandgap structures are generally engineered periodic or non-periodic arrangement of unit cells helps to stop or assist propagation of electromagnetic waves for all incident angles in a particular frequency band.

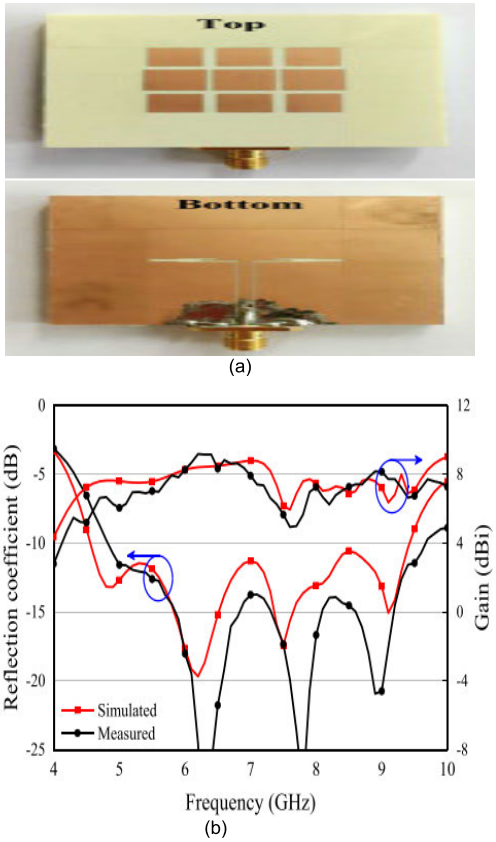

FIGURE 18. Antenna using metasurface to improve the gain and bandwidth of an antenna [128] (a) Antenna design (b) Reflection coefficient and gain.

Introducing EBG in antenna design results in low profile, suppression of surface waves, and high gain by acting as a transmission or reflection surface [130]. An EBG structure is developed on a square patch using an arrangement consisting of a cross-shaped slot with a fork-shaped slot in [131]. The proposed monopole antenna has a beveled Y-shaped structure as a radiating element and partial ground integrated with EBG provides wide bandwidth of 3.1-10.6 GHz and peak gain of 6.25 dBi with good radiation characteristics as shown in Figure 20. As the size of the fork slot is increased associated capacitance is increased and thereby bandstop response increases.

The gain enhancement of monopole antenna using high-frequency impedance is proposed in [132]. HIS suppresses surface waves and makes incident and reflected waves in phase. The existence small magnetic field on the surface leads to the high surface impedance at the resonating frequency. The developed fork-shaped monopole antenna is integrated with the HIS to achieve a bandwidth of 32.3% and gain of 4.5 dBi when compared to the antenna without HIS as shown in Figure 21. The FSSs are the periodic arrangement of unit cells exhibiting particular transmission and reflection characteristics when an electromagnetic wave travels from it. FSS structures are developed either by using metallic patches or apertures on a metallic surface. The metallic patch FSS

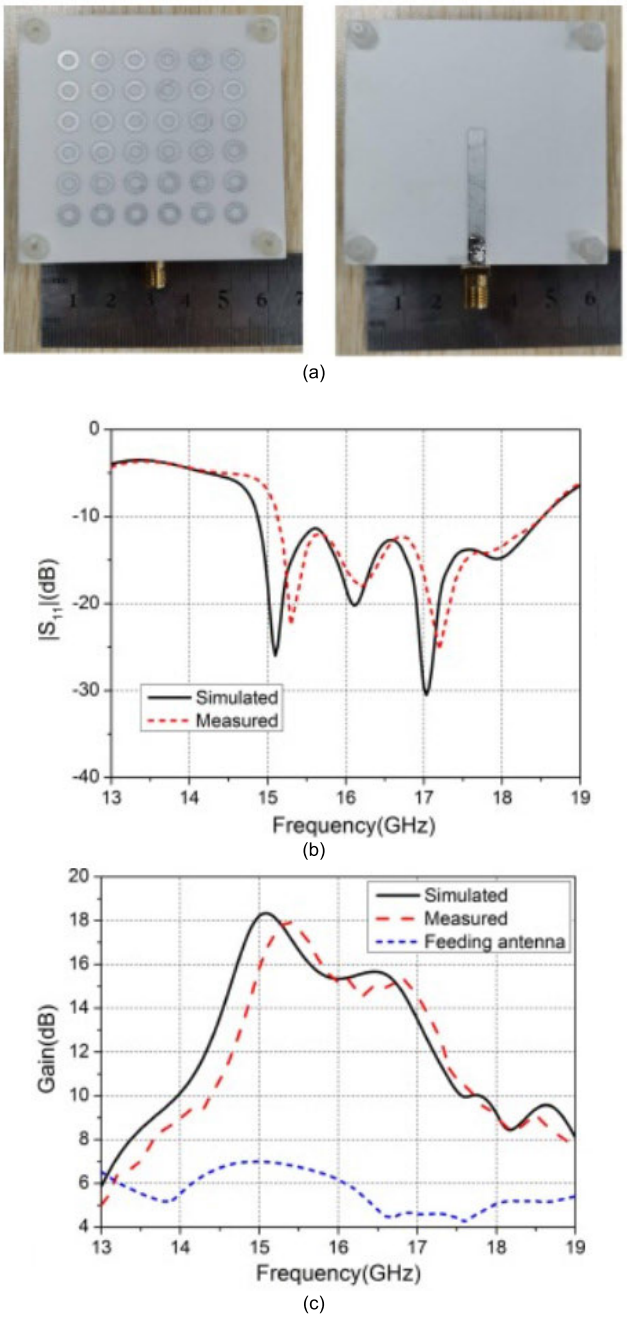

FIGURE 19. Antenna using PRS to improve the gain and bandwidth of an antenna [129] (a) Antenna design (b) Return loss and (c) gain.

shows capacitive behavior and acts as a low pass filter. On the other hand aperture-based FSS shows inductance behavior and acts as a high pass filter. The antenna with FSS improves the gain and bandwidth of the antenna [133].

The literature shows FSS can be used to design AMC such as HIS, EBG to improve the performance of the antenna. A bowtie dipole MIMO patch antenna is proposed in [134] using AMC loading to achieve high gain and bandwidth. In this proposed antenna V-shaped parasitic patches are placed along with the bowtie antenna to generate two resonance modes as shown in Figure 22. AMC ground plane is placed

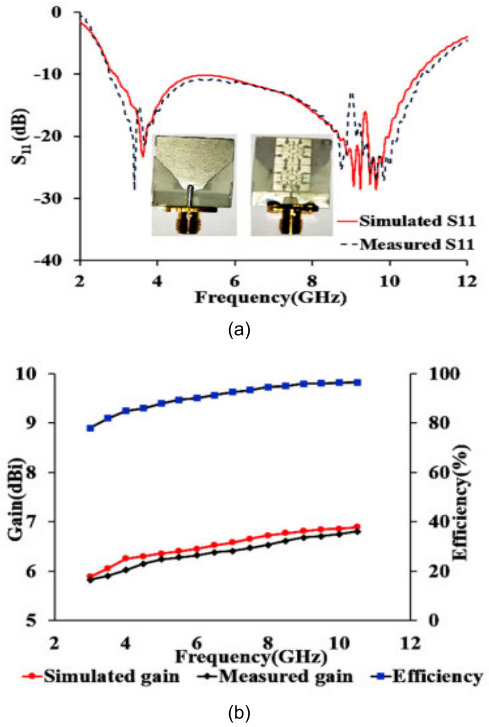

FIGURE 20. Antenna using EBG to improve the gain and bandwidth of an antenna [131] (a) Antenna design (b) Gain and efficiency.

below the radiating patch at a distance of 10.5 mm rather perfect electric conductor (PEC) ground plane to enhance gain with a low profile. The proposed design reported a peak gain of 7.1 dBi, impedance bandwidth of 31% (3.0 to 4.1 GHz), and port isolation of greater than 25 dB.

D. CRLH/RESONANT DISPERSION

Numerous MTM structures are used in gain and bandwidth enhancement such as epsilon and mu negative materials, double negative materials, AMCs, SRRs, and CSRRs, etc. Composite right and left-handed structures are also one of the MTM structures used for enhancing the performance of the antenna. Development of CRLH includes an interdigital/meander line to form a capacitor and a shorted stub to form inductance. The proper tuning of CRLH dimensions especially shorted stub inductors improves the gain of the antenna. In [135] open ended ZOR based dual-band antenna is proposed for gain and radiation characteristics improvement. This proposed design uses an AMC reflector below the CRLH-TL of the antenna having a shunt element as a closed ring resonator reports a peak gain of 7.1 dBi and radiation efficiency of 89% at 3.52 GHz frequency. The placement of the AMC reflector improves the gain as the distance increased there will be better impedance matching. The bandwidth of an antenna is improved by loading the CRLH unit cell is due to the existence of a zeroth-order resonator, first-order positive resonator, and first-order negative resonator (FONR). The proper alteration of shunt and series inductance and capacitors i.e., LC equivalent circuit of CRLH-TL, mode coupling

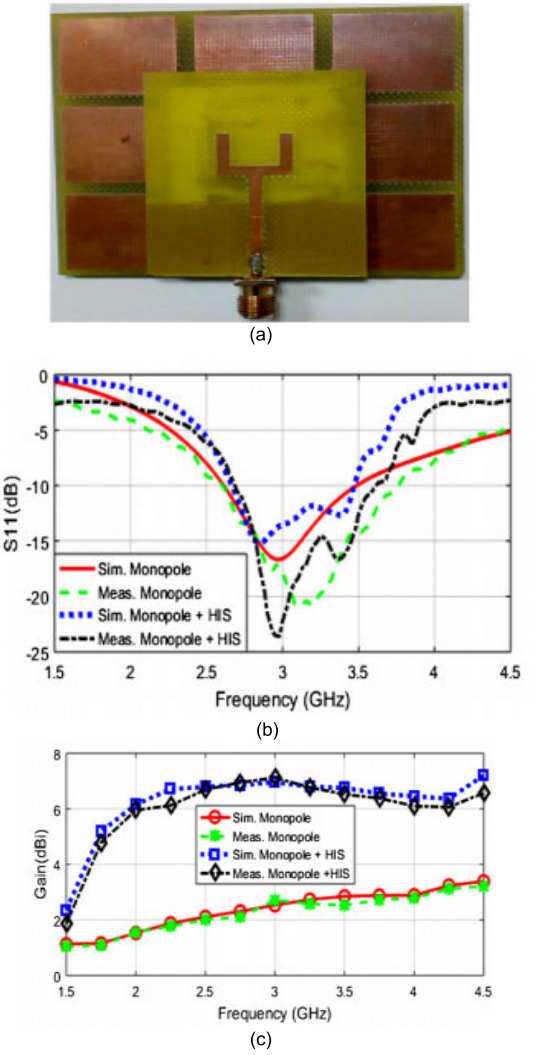

FIGURE 21. Monopole antenna with HIS [132] (a) Antenna design (b) Return loss (c) Gain.

techniques such as merging ZOR, FOR, and FONR behave as single passband resulting in wider bandwidth. Conversely, the gain of an antenna can be improved by embedding SRR and CSRR structures with CRLH [136]–[141]. In [142] developed an antenna based on CRLH unit cell for enhanced bandwidth of 71.11% and maximum realized gain of 3.75 dBi and gain by merging ZOR and FOR as shown in Figure 23.

In [143] asymmetric coplanar waveguide antenna is proposed by using a combination of CRLH-TL and modified ground plane to enhance bandwidth as shown in Figure 24. This developed antenna has a bandwidth of 109.1% by forming series and shunt capacitance on the patch. Interdigit or meander line structure forms series capacitance.

E. SUMMARY

The conventional patch antenna suffers from low gain, narrow impedance bandwidth, a stimulus of surface waves, and less efficiency. These antenna performance metrics can be enhanced by designing an MTM influenced antenna.

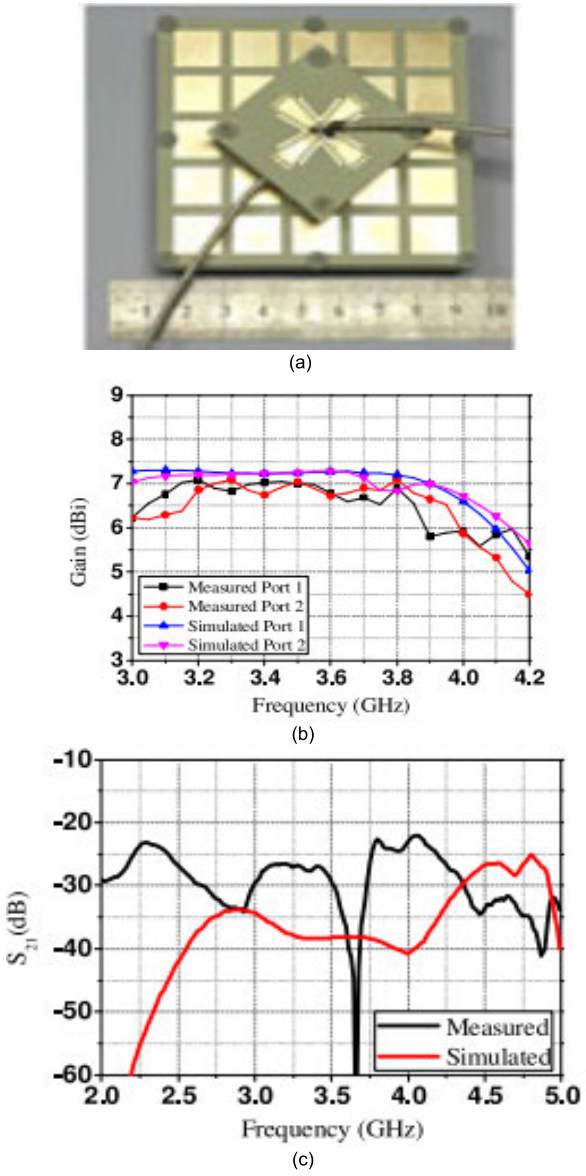

FIGURE 22. A wideband, low profile, and enhanced gain patch antenna using AMC as a ground plane [134] (a) Antenna design (b) Gain (c) Return loss.

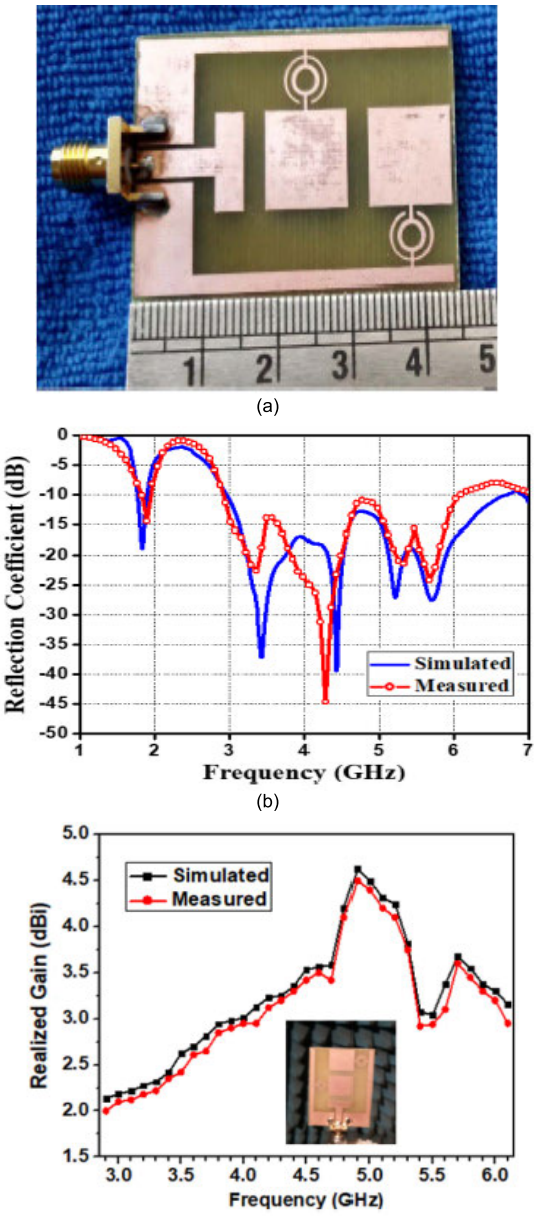

FIGURE 23. Antenna based on CRLH-TL for gain bandwidth improvement [142] (a) Antenna design (b) Reflection coefficient (c) Realized gain.

The DNG MTM-based antenna enhances radiated power. The antenna developed on high permittivity material improves gain i.e., higher the permittivity of a material higher is the gain. Photonic crystals are of high dielectric material with a low dielectric material such as air holes which confines electromagnetic waves in all directions. The increase in the radius of the air hole in photonic crystals shifts zero-dispersion to a shorter wavelength and thus resulting in faster data communication applications. Incorporating filter characteristics in the antenna by using capacitive and/or inductively coupled loop resonator wider bandwidth and stable gain can be achieved. As capacitive and/or inductively coupled loop resonator acts as a near field resonant parasitic element for the antenna system. The SRR and CSRR are constructed by a nonmagnetic metal having different structures such as circle, square, hexagonal, etc. with a gap between them. The arrangement is equivalent to an LC circuit and variations of LC values ensuing in low radiation losses. The one, two, or three-dimensional structures consisting of a periodic sub-wavelength unit cell in association with the antenna allows manipulation of electromagnetic waves within the antenna system. This manipulation of electromagnetic waves helps to improve the gain and bandwidth of an antenna. Even the material exhibiting both right-handed and left-handed material characteristics is used to enhance the gain and bandwidth of the antenna by generating a zeroth-order resonator and first positive/ negative order resonator. The aforementioned various techniques to enhance gain and bandwidth are summarized and similar techniques are listed in Table 5.

TABLE 5. Gain and bandwidth enhancement of an antenna using MTM.

Ref	MTM technique	Dimension, λ_0	S_{11} bandwidth, % / BW enhancement	Max gain, dBi	Radiation efficiency, %	Directivity, dBi
[144]	Mu negative MTM unit cell	0.24×0.24×0.001	52	4.8	-	-
[145]	MTM structure	2.64×1.48×0.058	30.6	9.2	73	-
[146]	TZ-shaped MTM resonator array	0.32×0.3×0.07	2.99 / -	5.39	93	6.71
[147]	Very large epsilon material	0.021×0.018×0.001	17.8, 35.8 / -	-17.1, -9.81	-	-
[148]	Mu negative MTM unit cell	0.25×0.29×0.002	34	4.5	-	-
[149]	Ring slot	0.139×0.139×0.015	1.58	-1.28	48.2	1.95
[150]	MTM superstrate with SRR and wire strips	1.01×1.29	- / 89	12.1	-	-
[151]	partially reflective surface as a superstrate	1.28×0.15×0.067	15.5	13.78	-	-
[152]	U-shaped metallic reflector	0.48×0.35×0.006	62.6	6.8	-	-
[153]	Hexagonal ring electromagnetic bandgap (EBG)	0.517×0.517×0.055	18	5.93	-	-
[141]	CRLH-TL	0.241×0.267×0.013	139.19	6	86.84	-
[142]	CRLH-TL	0.43×0.29×0.015	71	4.5	>61	-
[143]	CRLH-TL	0.32×0.19×0.015	109	3.37	65	-
[154]	CRLH-TL	0.13×0.08×0.009	173, 169, 158, 158 / -	3, 3.4, 4.4, 4.7	-	-

- Not available

V. IMPACT OF MTM TO ACHIEVE CIRCULAR POLARIZATION

The antenna is a transducer element that converts electric current into EM waves at radio frequency and radiates it into free space. One of the essential concern while choosing and establishing an antenna is its polarization. Wireless communication system adopts either linear (vertical/horizontal) or circular polarization (CP) based on the application requirement. In linear polarization, the electric field is perpendicular (vertical) or parallel (horizontal) to the surface conversely, in circular polarization EM waves rotate in a plane perpendicular to the direction of the wave. The circularly polarized wave can rotate in two ways if it is clockwise referred to as right-hand circular polarization (RHCP) and anticlockwise referred to as left-hand circular polarization (LHCP). Circular polarization antennas provide many merits when compared to the linear polarization antennas like absorption, reflectivity, solves phasing issues, combating fading or multipath interferences, resistance to inclement weather, and provides flexibility in antenna orientation. These merits emphasize CP antennas in applications such as wireless sensors, mobile and satellite communications, radio frequency identification, and wireless local area network, and more. The significant key parameter for assessing CP of antennas are axial ratio (AR) and surface current distribution. The AR is the ratio of the major to the minor axis of an ellipse polarization and is required to be 0 dB for circular polarization but practically it should be below 3 dB [155]. The literature reports different approaches to achieve circular polarization such as disrupting the radiating surface [156]–[159], stack arrangement in antenna [160], introducing switching element in antenna [161], reorganizing feeding network [162], using magnetoelectric dipole [163], using loop antennas [164], etc. This section mainly describes the role of metamaterial in realizing an antenna having CP characteristics.

A. MTM LOADING

The loading of different MTM structure in association with an antenna will provide robust CP characteristics in the operating bandwidth of the antenna. In [147] circularly polarized antenna is developed to operate in the ISM band (915 MHZ and 2450 MHz) using an MTM structure. The unit cell of the MTM structure is constructed by a 2×2 H-shape etched plane on a high dielectric permittivity material as a superstrate. This configuration improves the gain and AR of the antenna as shown in Figures 25a and b. This is because of high dielectric superstrate acts as a decoupling element between the antenna and its surrounding lossy environment. The MTM structure

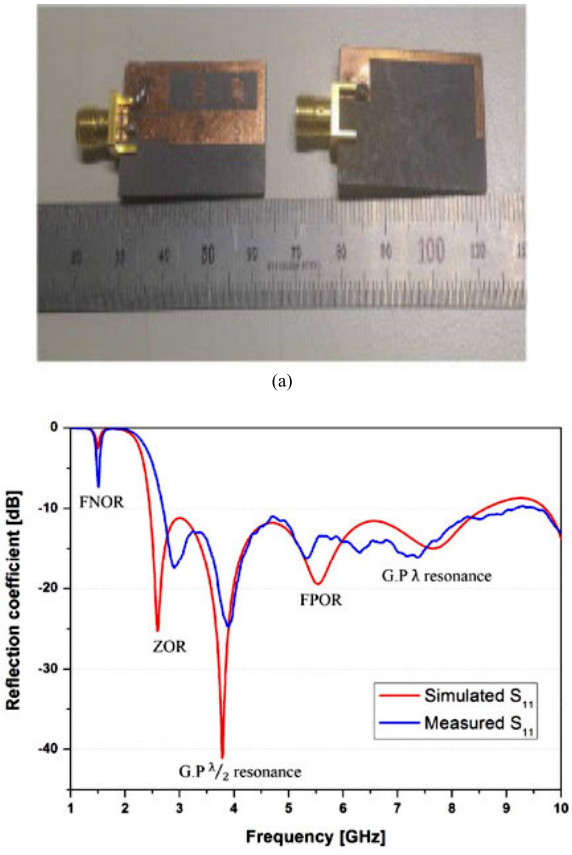

FIGURE 24. Antenna based on CRLH-TL and modified ground plane for bandwidth enhancement [143] (a) Antenna design (b) Reflection coefficient.

increases the effective aperture of the antenna by improving field distribution resulting in enhanced AR bandwidth. This proposed antenna demonstrates LHCP behavior as shown in Figure 25c. At the operating frequency, the substantial current density is upward and towards the right for 0^0 and 90^0 phase respectively. The phase 180^0 and 270^0 has current distribution as same as 0^0 and 90^0 but in the opposite phase.

The antenna system comprised of electric monopole and large capacitively-loaded loop (CLL) NFRP elements provides desired circular polarization. The ground plane based NFRP antennas is inappropriate for CP because it radiates only in one direction i.e., linear polarization. For CP, large CLL NFRP elements are arranged in such a way that it should behave like a magnetic dipole and radiates LP vertical to it [165]. Using this concept an NFRP based antenna is proposed in [166] for CP characteristics. It consists of two monopole antennas with a single coaxial feedline loaded with two orthogonal CLL with similar configuration positioned vertically with regards to the ground plane demonstrates good AR and radiation efficiency as shown in Figure 26. A patch antenna with CP behavior is developed in [167] using anisotropic high refractive index (HRI) MTM structure. The anisotropy property of HRI MTM creates the phase difference in orthogonal components. By rotating the unit cell structure RHCP or LHCP can be realized.

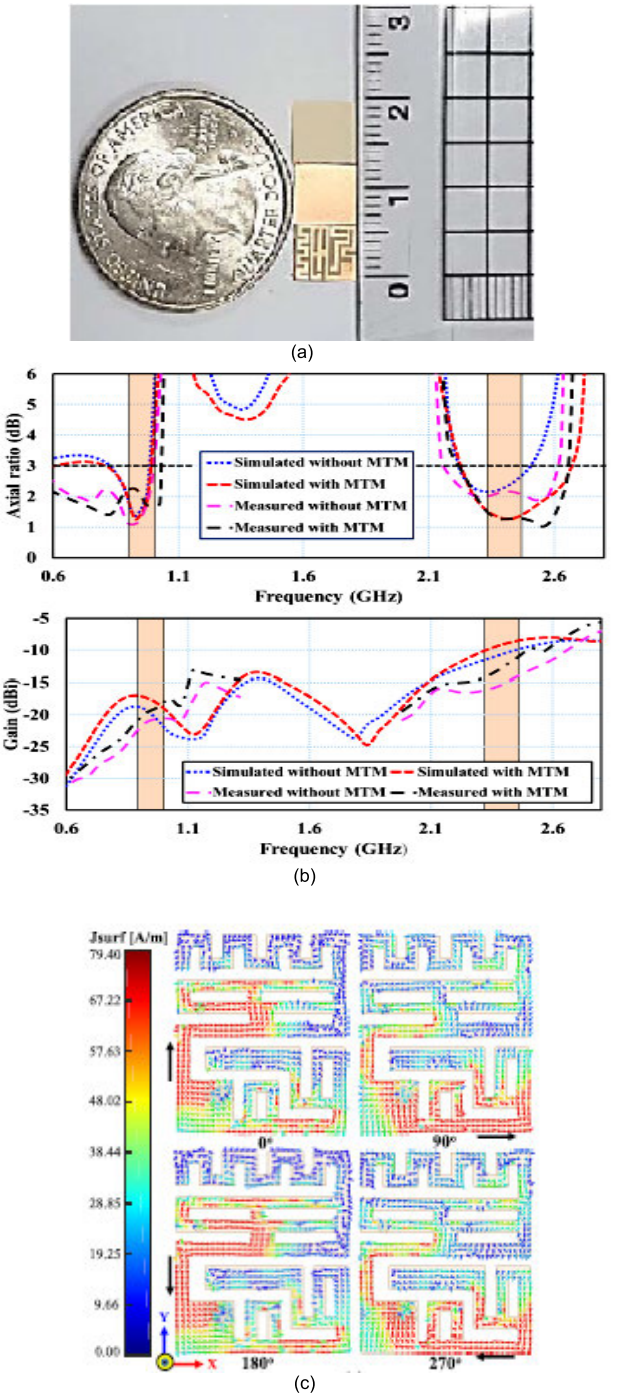

FIGURE 25. MTM structure loaded antenna to achieve circular polarization [147] (a) antenna design (b) Gain and AR (C) Surface current distribution.

B. MTM INSPIRED ANTENNA

The CP of an antenna generally depends on antenna geometry and the elements positioned on it. The SRR and CSRR MTM structures are also used to achieve the CP behavior of an antenna. In [168] proposed a CP antenna for satellite application based on SRR and CSRR MTM structures. This antenna modified ground plane and radiating stubs for impedance matching with coplanar waveguide feeding as

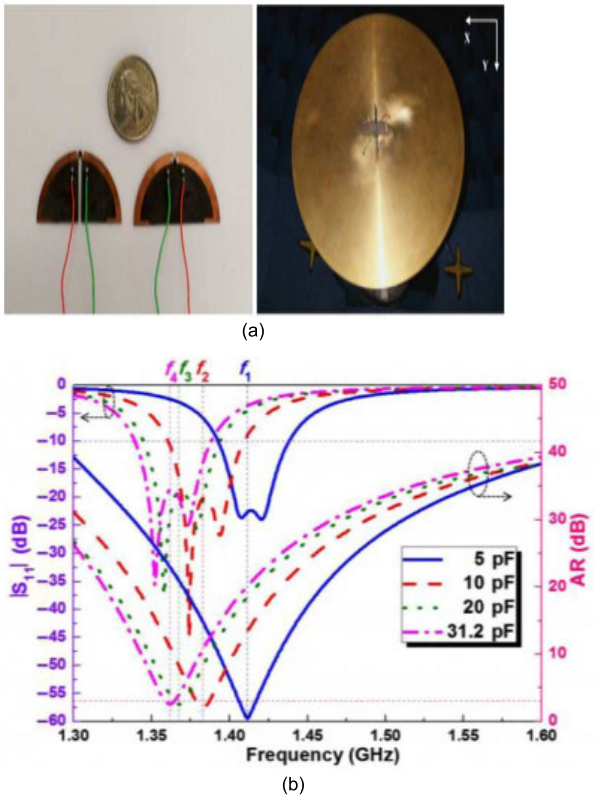

FIGURE 26. NFRP antenna demonstrating CP [166] (a) Antenna design (B) S-parameter and AR with respect to frequency.

shown in Figure 27a. The introduction of SRR and CSRR structures on antenna elements varies the effective inductance and capacitance of the antenna and affects the orientation of current distribution which helps in achieving CP as shown in Figure 27c.

C. METASURFACE LOADING

Apart from the above-mentioned metamaterial techniques to achieve CP metasurface loading is also a significant approach to achieve CP as well as improving other antenna parameters such as miniaturization, gain, bandwidth, etc. metasurface loading consists of HIS, RIS, EBG, FSS, and so on. In [169] proposed an antenna using a 9 × 9 zero index MTM (ZIM) unit cell structure as shown in Figure 28a. The ZIM is realized using a square shape unit cell with two asymmetric split gaps that provide zero or near-zero permittivity and permeability. The split gap on the square unit cell creates two orthogonal electric field components responsible for CP and this structure reports good gain and axial ratio bandwidth.

The RIS constructed by 4 × 4 metal patches is used to increase the AR bandwidth of the antenna proposed in [170]. The H-shape perturbed radiating patch in proposed provides CP behavior. The RIS is placed in between the radiating patch and ground plane. The RIS layer uniformly distributes image current and helps in reducing mutual coupling between the antenna current and its image. The inductive reactance of

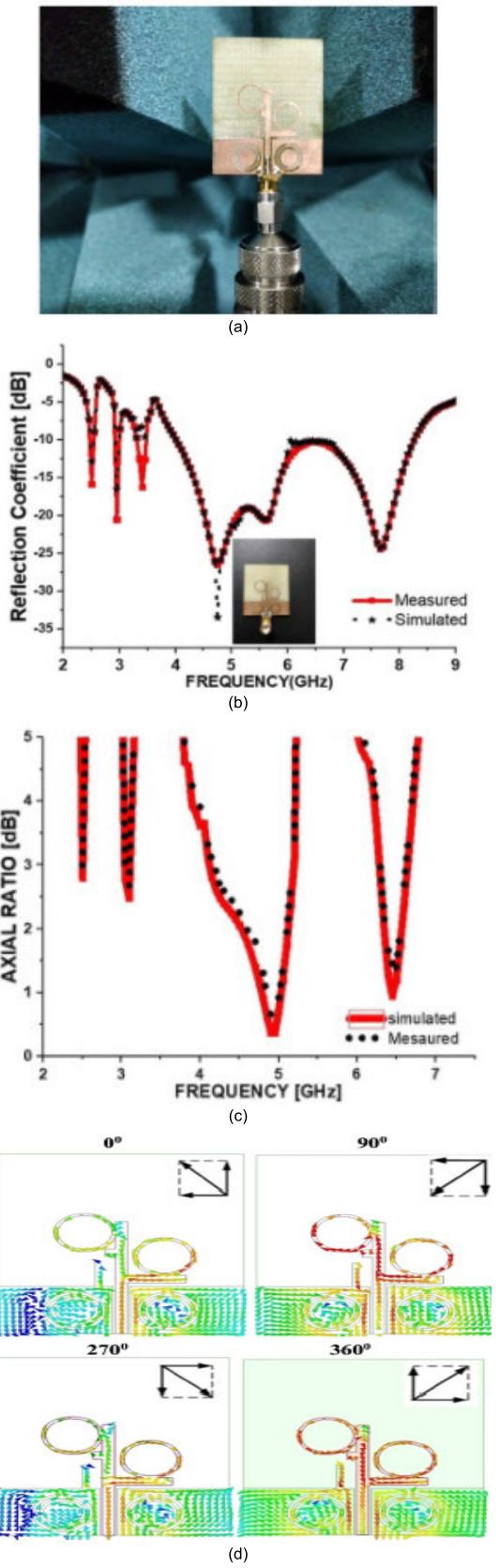

FIGURE 27. SRR and CSRR based antenna [168] (a) antenna design (b) reflection coefficient (c) AR and (d) Surface current distribution at 2.5 GHz.

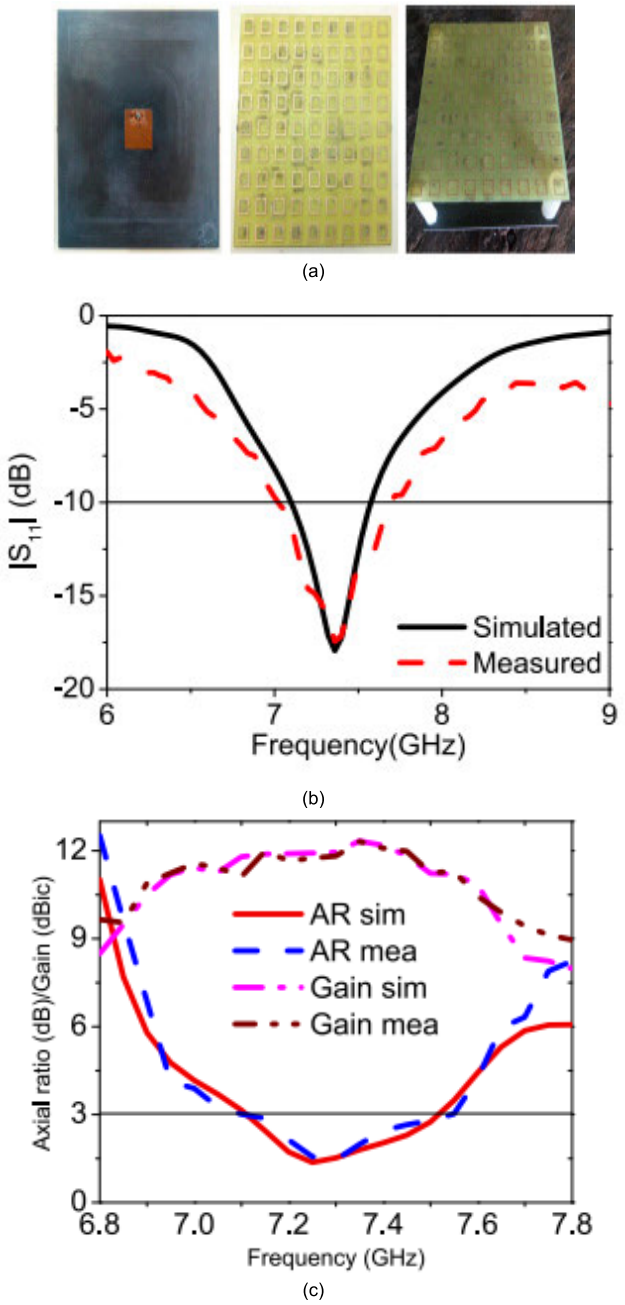

FIGURE 28. CP antenna with ZIM loading [169] (a) antenna design (b) S-parameters and (c) AR.

the RIS surface neutralizes near field capacitive effect on a radiating patch and thereby resulting in compact and wider AR bandwidth. The EBG metasurface suppresses a surface wave and in phase characteristics make it behave like an artificial magnetic conductor. These properties of EBG helps in enhancing antenna performance parameters.

D. CRLH/RESONANT DISPERSION

The composite right/left-hand medium supports to achieve CP behavior of an antenna apart from antenna miniaturization, enhancement of gain and bandwidth, mutual coupling suppression in the MIMO antenna system. The development of CRLH includes an interdigital/meander line to form a capacitor and a shorted stub to form the inductance as discussed in the previous section. The surface current of an antenna decides the polarization characteristics of the antenna. The meander lines and shorted stubs disturb the current distribution of an antenna and establish two orthogonal modes with 90^0 shift. In [171] proposed a CP antenna based on CRLH. The proposed antenna consists of two uneven meander lines located between the patch to act as shunt inductance and two slots are engraved to form a series capacitance as shown in Figure 29. This effective inductance and capacitance perturbs the current distribution and creates two orthogonal modes with a phase difference resulting in circular polarization.

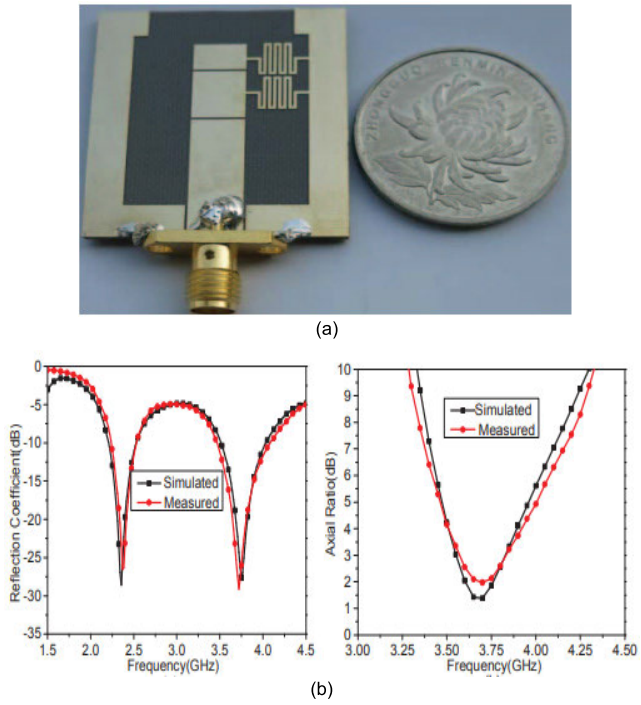

FIGURE 29. CP antenna based on CRLH [171] (a) antenna design (b) reflection coefficient and AR.

E. SUMMARY

Antenna polarization characteristics is one of the most essential features required in modern communication system. Polarization of the antenna can be linear or circular and is ascertained by its electric field orientation. The reciprocity property of an antenna demands transmitter and receiver antenna orientation same otherwise there will be huge signal loss due to cross-polarization. This effect is valid for an antenna having linear polarization. Conversely, in circular polarization, the EM field rotates circularly covering vertical, horizontal, and all the planes between them. This feature provides many advantages over linear polarization antenna as listed in the earlier section additionally 3dB increased signal strength as CP antennas are immune to the Faradays rotation

effect. Implementation of such CP antennas using MTM is demonstrated. The MTM structure exhibits resonance characteristics, facilitates variation of effective inductance and capacitance of the antenna system. By choosing appropriate geometry, MTM structure and feeding of an antenna cause a change in reactance and affects the surface current distribution of an antenna structure. this process helps in achieving CP characteristics in the antenna as well as antenna miniaturization and enhanced bandwidth. The Table 6 summarizes the aforementioned CP antenna and also selected similar CP antenna performance parameters such as resonant frequency, feed type, gain, AR bandwidth, number of bands.

VI. SUPPRESSION OF MUTUAL COUPLING/ISOLATION ENHANCEMENT IN MIMO ANTENNA USING MTM

A low correlation coefficient accounts for suppression of mutual coupling in MIMO antenna systems which directly influences the impedance matching of the antenna systems and mutual coupling between the multiple antenna elements in the MIMO system. The high mutual coupling between the adjacent elements in the MIMO systems degrades the performance of diversity parameters such as envelope correlation coefficient (ECC), diversity gain (DG), total active reflection coefficient (TARC), mean effective gain (MEG), multiplexing efficiency (ME), and channel capacity loss (CCL). The channel capacity in MIMO systems improves with the increase in the antenna element. Conversely, due to the compact space allocated for antennas in electronic gadgets, the antenna should be placed close to one another. If the spacing between antenna elements is less than $\lambda/4$, resulting in high mutual coupling or low isolation. Hence suppression of mutual coupling in the MIMO antenna system is an important issue in the design of the MIMO antenna system.

The literature reports various approaches to suppress mutual coupling in the MIMO system such as decoupling network, defected ground structure, current localization, neutralization line, inserting parasitic elements, antenna placement and orientation, and so on as shown in Figure 30 [181]–[186]. Besides MTM-based antenna is also one significant approach to enhance isolation of the MIMO systems as shown in Figure 31.

The utilization of MTM structures in the MIMO antenna system disturbs the current distribution and behaves as a decoupling element between the adjacent antenna elements. Resonating behavior of MTM structures confines the magnetic field within the excited antenna and thereby suppresses mutual coupling.

A. MTM LOADING

To reduce mutual coupling in the MIMO system different MTM structures are loaded into the antenna which suppresses or absorbs excited waves from adjacent elements. A MIMO antenna system consisting of four elements is proposed in [187] using an MTM structure to enhance isolation between the nearby antennas. A mushroom-shaped wall is placed between the antenna elements resulting in an

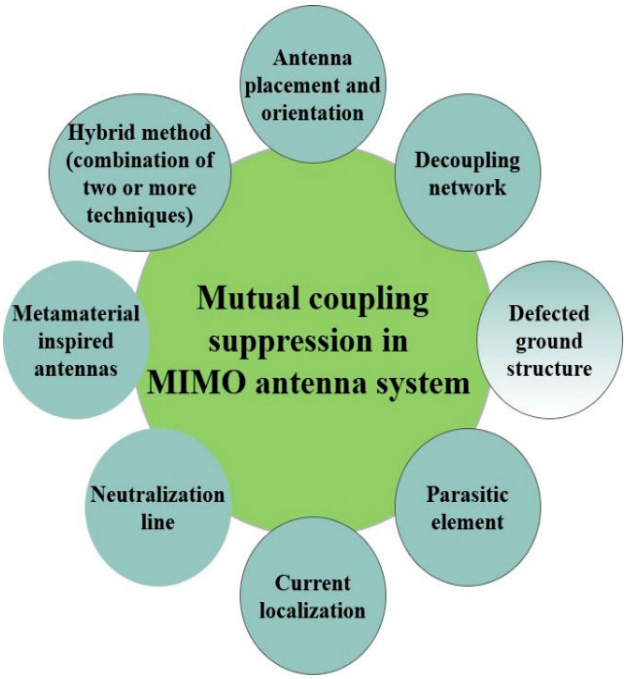

FIGURE 30. Different decoupling techniques for isolation enhancement in MIMO antenna systems.

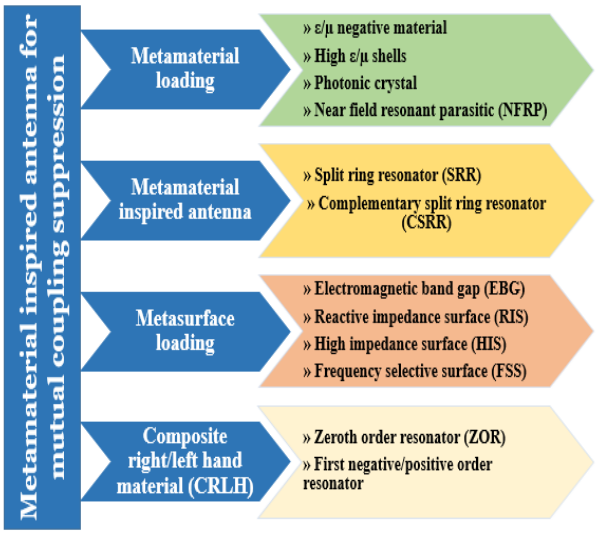

FIGURE 31. MTM based decoupling techniques for isolation enhancement in MIMO antenna system.

ECC of 0.02 across the frequency of operation and isolation enhancement between the antenna pair greater than 42 dB as shown in Figure 32. In the aforementioned design when antenna 1 radiates an electromagnetic wave that couples to antenna 2. These coupling waves are suppressed by the mushroom wall structure exhibiting bandstop characteristics.

In [188] proposed a MIMO antenna system using circle-shaped near-zero permittivity and permeability MTM as a decoupling technique as shown in Figure 33. The proposed MIMO antenna demonstrates maximum isolation of 41 dB with a correlation coefficient of less than 0.26 within the

TABLE 6. Different MTM approaches to achieve CP characteristics.

Ref	MTM technique	Frequency (GHz)	Feed type	Gain	AR bandwidth (%)	Number of bands
147	H-shaped etched 2×2 MTM structure with Epsilon very large superstrate	0.915, 2.450	Coaxial	-17.1, -9.81 dBi	21.3, 17.4	two
166	Frequency agile NFRP	1.39	Coaxial	5.93 dB	3.92	single
167	HRI SRR MTM	2.03	Coaxial	-3.1 dB, -3.05 dB	2.1	single
168	SRR and CSRR	2.47, 3.08, 4.5, 6.47	Coplanar waveguide	4.8 dB	0.1,0.1,1.15,0.5	quad
169	Zero indexed MTM	7.45	Coaxial	12.31 dBic	6.87	single
170	RIS	5.5	Probe	7.2 dBi	27.5	single
171	CRLH	2.35, 3.65	Coplanar waveguide	5.60 dBi	9.7	two
172	SRR and CRLH-TL	3.30	Microstrip line	5.4 dBic	14.1	single
173	Mushroom type MTM	5.2	reconfigurable	8.2 dBi	28, 30.3	single
174	FSS	20.67,29.71	Coaxial	-	5.56,3.97	two
175	EBG	5.63	Microstrip line	13 dBic	22.5	single
176	4×4 periodic metal plate metasurface	5.55	Coaxial	7.6 dBic	23.4	single
177	4×4 square shape metallic patch	2.15	Microstrip line	7 dBic	31.3	single
178	Diamond shaped metasurface	9	-	12 dBic	37.6	single
179	Partial reflective surface	5.77	Coaxial	17.3 dBi	2.5	single
180	EBG	3.32, 6.22	Coaxial	-	2.4,3.5	two

operating frequency band. The Refractive index of epsilon mu near zero is approximately equal to zero and offers no phase variation in electromagnetic waves within the superstrate. This property epsilon mu near-zero helps to retain the original antenna radiation characteristics. ε near zero and μ near-zero offers to decouple near coupled electromagnetic field.

The near field resonators (NFR) can also be used in the MIMO antenna for enhancement of isolation between the antennas. In [189] NFRs are placed above the radiating patch to achieve isolation better than 20 dB as shown in Figure 34. The electric field distribution of antenna 1 is confined to only antenna 1 by producing orthogonal coupling mode at the operating resonant frequency. A substrate of the antenna behaves as transmission media. The magnetic field will develop around the arrangement between the patch on the substrate and air. Because of the common substrate used for multiple radiating patches, the magnetic field of antenna 1 will couple to the adjacent antenna by substrate and air. As it can be seen from the current distribution figure antenna without NFR has strong coupling between the antennas.

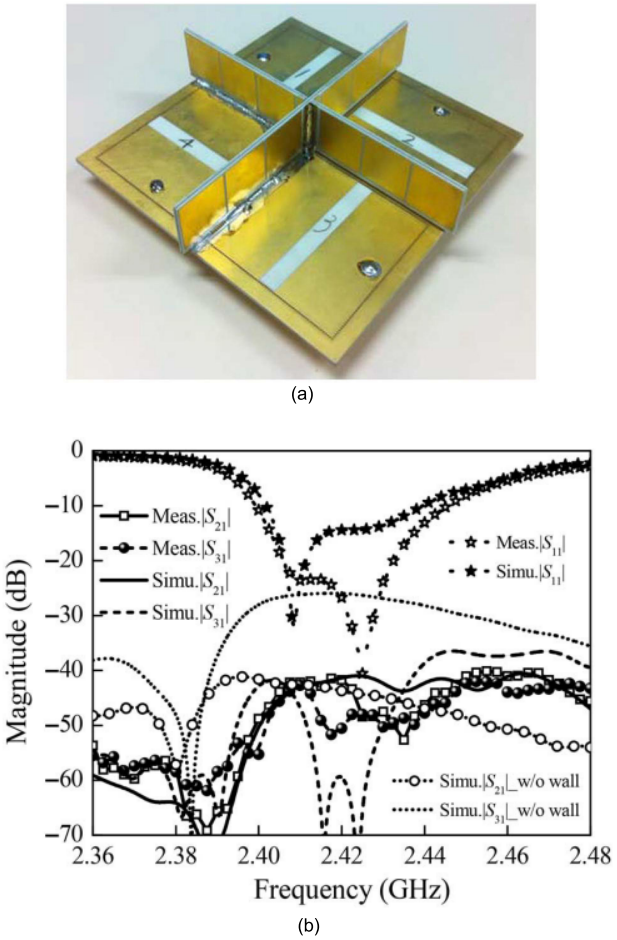

FIGURE 32. Four-element MIMO antenna with mushroom wall MTM loading for enhancement of isolation [187] (a) Antenna design (b) Return loss.

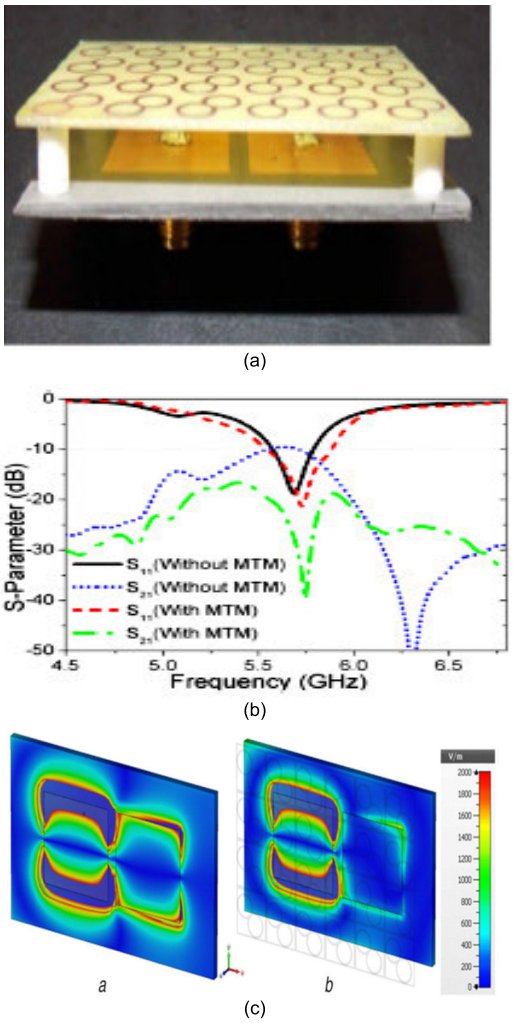

FIGURE 33. Four-element MIMO antenna for isolation enhancement using MTM superstrate and E-field distribution when port 1 excited with and without MTM [188] (a) Antenna design (b) S-parameter (c) Current distribution in MIMO antenna.

The antenna with NFR antenna 1 and NFR on it has strong current distribution whereas antenna 2 and NFR on it is very weakly coupled. Therefore, placing NFR above the patch will restrict the magnetic field loop within the excited antenna element.

B. MTM INSPIRED ANTENNA

To enhance isolation between the MIMO antenna SRRs and CSRRs structures (not limited to the only split ring, a structure may be of square, hexagonal, etc.) are widely used in antenna design. In [190] Vivaldi antenna with a microstrip feed line is proposed and to suppress mutual coupling between the antenna elements triple band gap CSRR is used as shown in Figure 35. This structure is placed parallelly between two Vivaldi antenna arrays, due to bandstop characteristics of CSRR mutual coupling between the antennas is reduced. A simple and effective improvement of the isolation structure is proposed in [191]. The proposed design has four antenna elements incorporated with the CSRR to operate in the ISM band as shown in Figure 36.

C. METASURFACE LOADING

The arrangement of multiple antennas in a compact size is the need for a modern wireless communication system. For the improvement of channel capacity, multiple antennas are deployed at transmitter and receiver, it utilizes multipath signal propagation. Multiple antennas resulting in a decrease of overall gain of the system due to cross talk. As discussed in the aforementioned section excitation of substrate mode plays a significant role in the mutual coupling between the antennas fabricated on a single substrate [192]–[193]. To reduce mutual coupling one way is to be loading the antenna with metasurfaces.

The electromagnetic bandgap structures are composed of an array of subwavelength structures that behaves like an array of a band-stop filter at the operating frequency of an antenna and confines propagation of surface waves within the antenna. In [194] reported a multiple antenna system using split EBG to suppress mutual coupling and meander line to achieve dual-band as shown in Figure 37. The EBG structures are constructed by subwavelength metallic patches with their edges connected to a neighboring element by a metallic strip in an interdigital shape. The four splits are

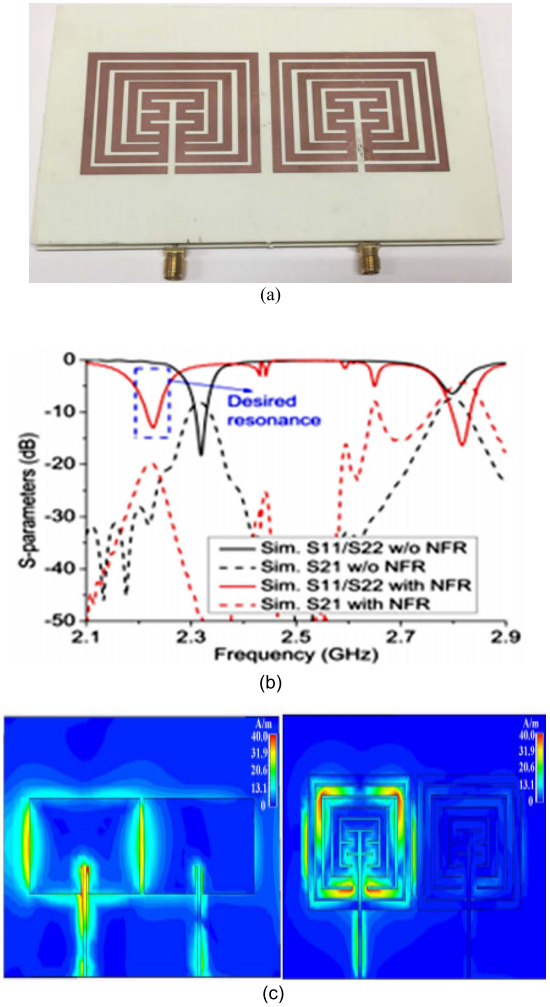

FIGURE 34. Two-element MIMO antenna for isolation enhancement using NFR and current intensity of two-element MIMO antenna without and with NFR [189] (a) Antenna design (b) S-parameter (c) Current distribution in MIMO antenna.

created on the EBG to eliminate coupling current propagation at the first resonance mode and the EBG structure behaves as coupling decoupling eliminate at the second resonance mode. Two main sources of mutual coupling are firstly the return current at the ground plane, eliminated by inserting the EBG ground plane between two antennas. The second source is surface current at the top plane and is suppressed by creating a high impedance surface of EBG. In [195] proposed a MIMO antenna to reduce direct coupling between the patches by separating two patches with the EBG of fractal shape as shown in Figure 37. The artificial magnetic conductor surface loading has similar characteristics to the EBG surface. The in-phase reflection and high impedance surface characteristics make AMC structures a significant candidate in antenna design. AMC surface restricts the propagation of surface waves in a normal electric field therefore loading AMC surface with antenna reduces mutual coupling and enhances the radiation performance of the antenna and broadband.

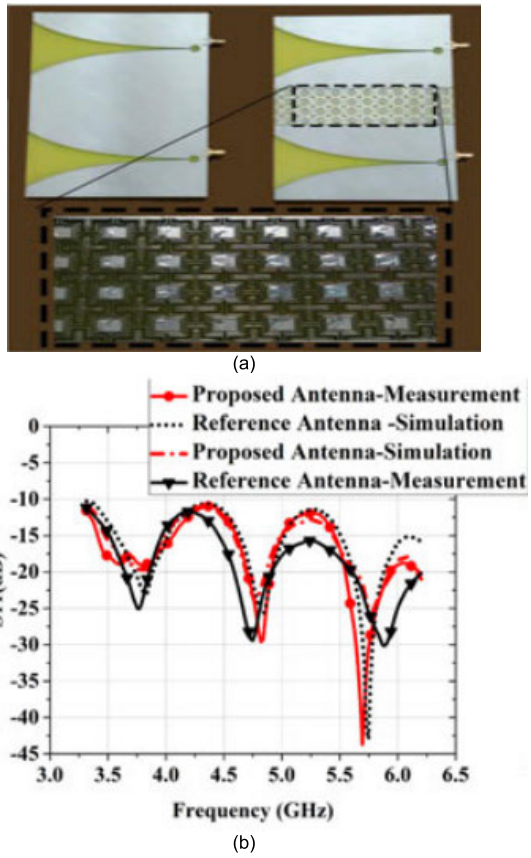

FIGURE 35. Two-element MIMO antenna for isolation enhancement using MTM loading [190] (a) Antenna design (b) Return loss.

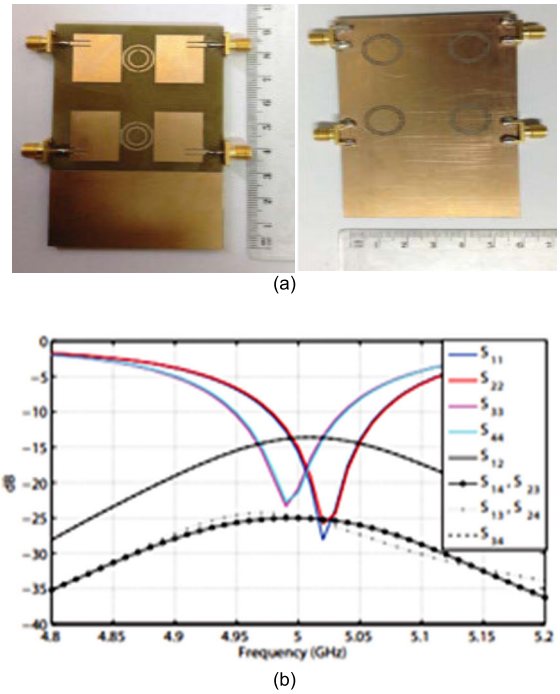

FIGURE 36. A 2 × 2 antenna system for isolation improvement using CSRR [191] (a) Antenna design (b) S-parameters.

The FSS loading at the ground plane, above the radiation patch, above and below the patch, and two or more layer of

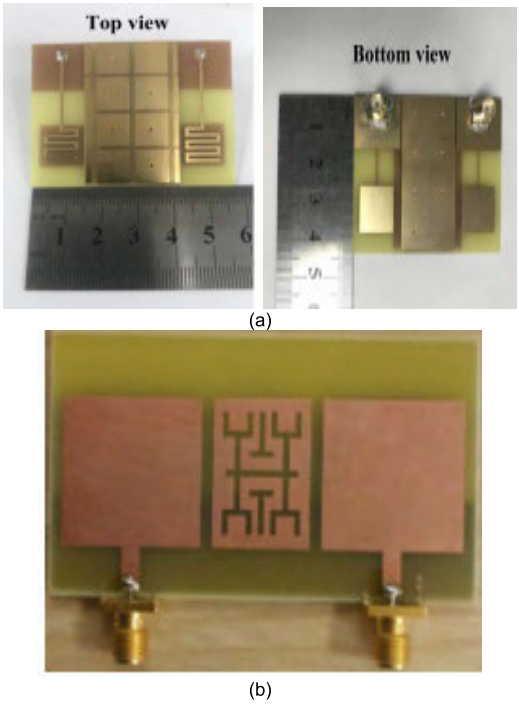

FIGURE 37. Antennas for mutual coupling suppression using EBG [194], [195] (a) Antenna design with metallic EBG (b) Antenna design with fractal EBG.

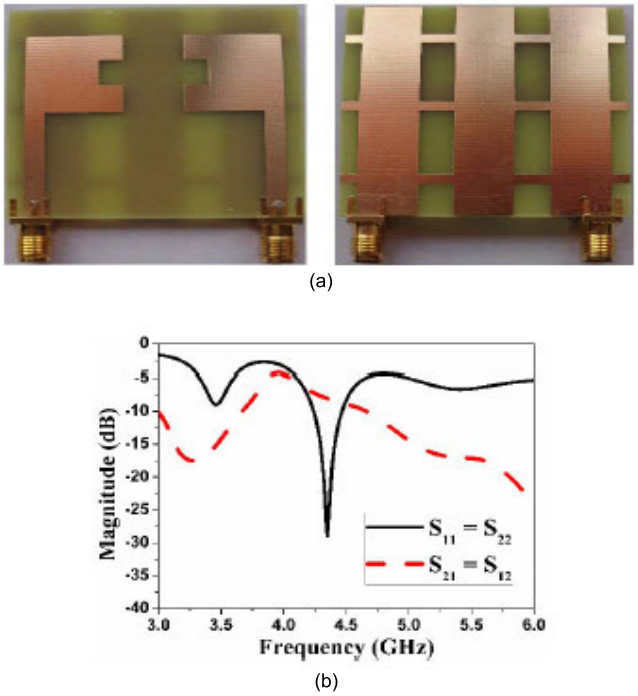

FIGURE 38. Two element MIMO antenna system based on FSS [196] (a) Antenna design (b) S-parameters.

FSS on top and/or bottom of the antenna as a superstrate reduces mutual coupling between the elements in MIMO antenna systems [196]–[198].

In [196] demonstrated a two-element MIMO system using FSS for improving isolation as shown in Figure 38. In this

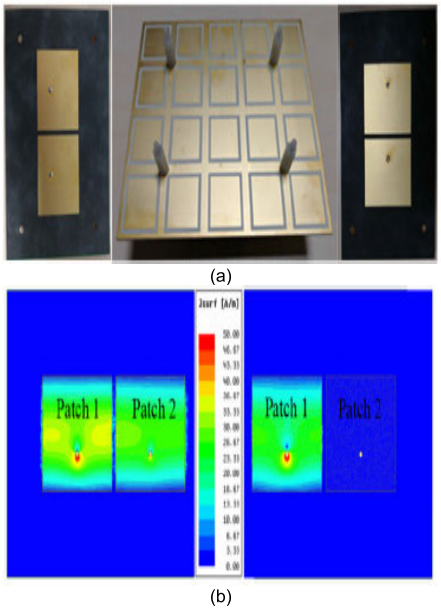

FIGURE 39. Antenna with metasurface loading [199] (a) H-plane (left) and E-plane (Right) coupled antenna design (b) Current distribution of H-plane without and with metasurface.

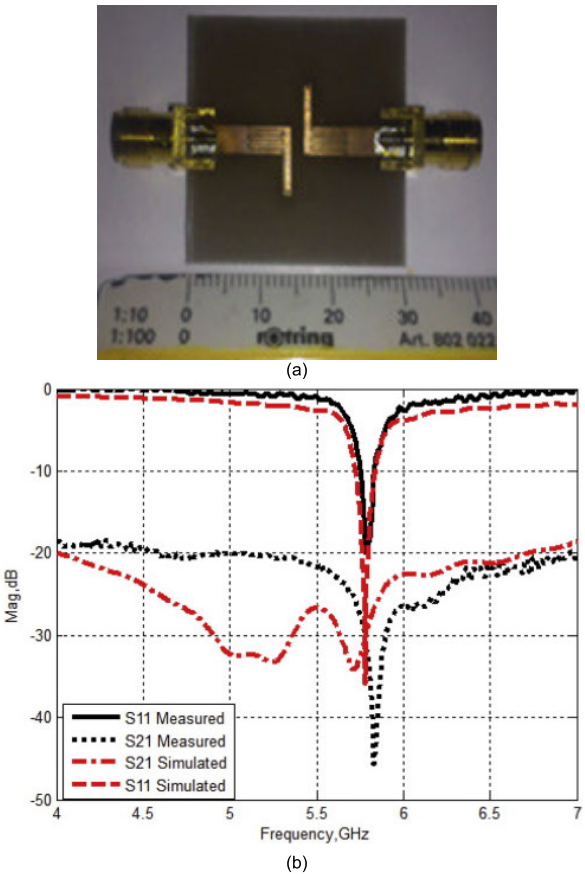

FIGURE 40. Two-element MIMO antenna with CRLH to improve isolation [200] (a) Antenna design (b) S-parameters.

proposed antenna a single layer FSS is loaded on the ground plane of the patch antenna such that most of the radiating patch is not backed. Loading FSS at the ground plane behaves

TABLE 7. Enhancement of isolation in MTM influenced MIMO antenna.

Ref	MTM approach for mutual coupling suppression	Isolation achieved (dB)	Diversity performance						G	H	I	Dimension, λ_0	elements
			A	B	C	D	E	F					
[201]	ENG MTM	>20	<0.0025	-	-11	-	<0.35	-	7	60	182	0.24×0.28×0.016	8
[202]	MTM loading	>25	<0.013	9.98	-10	<3	-	-	6.2	88	98.63	0.58×0.58×0.031	2
[203]	SRR	>20	0.001	10		-4	0.358	-1.5	6	-	182	0.42×0.42× 0.016	2
[204]	HRI	10	<0.03	-	-	-	-	-	-	-	22.2	2.4×1.4×0.042	2
[205]	FSS	>16	-	-	-	-	-	-	-	-	182	0.39×0.27×0.004	2
[206]	EBG	>15	0.015	9.95	-10	-	-	-	7	80	138	0.14×0.24×0.011	2
[200]	CRLH reversal configuration	35	0.0002	10	-40	-	-	-	-	-	1.55	0.57×0.50×0.031	2

- Not available, A-ECC, B-DG, C-TARC, D-MEG, E-CCL, F-ME, G-Maximum gain in dBi, H-radiation efficiency%, I-impedance bandwidth%

as the defects in ground plane structure and resulting in discontinuity of surface current between two antennas thereby mutual coupling is reduced.

The decoupling of E/H-plane simultaneously in the patch antenna using metasurface loading is proposed in [199]. The surface wave excitation for TM and TE mode at a cut-off frequency due to a dielectric substrate is given by equation (6)

$$\left.\begin{aligned} f_c &= \frac{mc}{2h\sqrt{\varepsilon_r - \varepsilon_2\mu_2}}, \quad m = 0, 1, 2, \ldots..(TM\ mode) \\ f_c &= \frac{(2m-1)c}{4h\sqrt{\varepsilon_r - \varepsilon_2\mu_2}}, \quad m = 0, 1, 2, \ldots..(TE\ mode) \end{aligned}\right\} \quad (6)$$

In the above equation $\varepsilon_r = \varepsilon_2\mu_2$ then cut off frequency is infinite and resulting in complete suppression of surface waves as shown in Figure 39. The FSS layer is constructed by unit cells on a metal layer with square slots as shown in Figure 39. H-plane decoupling is achieved by placing the FSS element on top of the patches in the near field region. E-plane decoupling is achieved by properly adjusting the length and height of the unit cell in an FSS element.

D. CRLH/RESONANT DISPERSION

The unique property of the anti-parallel group and phase velocity of composite right left-handed material delivers numerous advantages such as improving gain and bandwidth, miniaturization and enhancing isolation in antenna and other microwave devices [25]. A CRLH based MIMO antenna is proposed in [200]. The CRLH unit cell constructed in the proposed MIMO antenna by left-hand material consisting of an interdigital structure behaves as a capacitor and a stub connected to it as inductor as shown in Figure 40. A zero phase shift or zeroth-order resonance is achieved by properly tuning the dimension of the CRLH cell at the operating frequency of the antenna. Two antenna elements are fabricated on a single substrate separated by 1.8 mm with a reversal CRLH structure. The interdigital capacitor stub is reversed in antennas 1 and 2. This structure provides a reverse current concerning to excited antenna thereby it increases isolation.

E. SUMMARY

In MIMO antenna system design, it is very important to ensure acceptable isolation between the antenna elements otherwise mutual coupling between the antenna elements degrades the overall performance of the MIMO system. One prominent solution to overcome the problem of mutual coupling is the utilization of MTM in the MIMO antenna system. Different structures based on ENG, MNG, and DNG MTM loading on the antenna acts as a decoupling element and enhances isolation between elements. Placing a near field

resonator structure close to the antenna confines the magnetic field within the antenna. The bandstop characteristics of SRR and CSRR prevent coupling between the antennas. Different metasurface structure loading on top and/or bottom of the antenna element suppresses the surface waves and enhances isolation. Even CRLH structures are also used in antenna design to suppress mutual coupling by generating reverse current in comparison with the excited antenna element. Table 7 summarizes the aforementioned and similar techniques to enhance isolation in the MIMO antenna system and also illustrates the values of diversity parameters for various MTM approach to enhance isolation.

VII. CONCLUSION AND FUTURE DIRECTIONS

The inception of MTM opened a new dimension in antenna design because of its unique electromagnetic characteristics such as negative permittivity and permeability, negative refractive index, and its manipulation. On the other fold, the evolution of electronic gadgets reserves a compact area for antennas and looking for better performance. Cater to this need in recent year's MTM-inspired antennas are emerging as a prominent technology. Several different approaches are examined for MTM-based antenna, in specific i) MTM structure loading having an ε/μ negative material, high permittivity/permeability cell, photonic crystal, near field resonant parasitic ii) SRR and CSRR inspired antenna iii) FSS, EBG, HIS, and RIS metasurface loading and iv) CRLH transmission line based antenna. Although, there are numerous applications of MTM in antenna design, however, here we have discussed explicitly its recent progress in antenna miniaturization, enhancement of gain and bandwidth, and suppression of mutual coupling in MIMO antenna systems.

Antenna miniaturization can be achieved by inserting MTM unit cell structures on top of the patch and/or bottom of the ground plane. An array of periodic subwavelength unit cells commonly termed as metasurface placing onto the antenna will change effective inductance and capacitance of the antenna system resulting in miniaturization. Apart from antenna miniaturization, MTM based antenna is a promising technology for improving the gain and bandwidth of an antenna. These antennas allow altering electromagnetic wave properties and effective inductance and capacitance of the antenna system. Alteration of these parameters ensures an increase in gain and bandwidth of the antenna. Perturbation of surface current density by choosing the proper geometry and shape of the antenna gives circular polarization. One of the severe problems in MIMO antennas is a mutual coupling between the neighboring antennas. So, the introduction of MTM structures in MIMO antenna suppresses mutual coupling by confining electric and magnetic fields within the excited antenna.

Although there are several advantages of MTM based antenna it has some limitations such as the miniaturization of MTM structure saturates the resonance frequency and decreases in magnetic response at infrared and optical frequencies, difficult to manufacture in large volume, the structure of the antenna can not be changed during operation, the MTM substrates are bulky and lossy at microwave region and it hinders their use in wireless applications.

The research in MTMs is versatile and involves many subjects such as material science, physics, chemistry, electromagnetics, etc. Here, we discuss several significant directions in the antenna design field.

- ➢ Development of novel antenna for next-generation wireless communication systems which involves new frequency band and wide spectrum such as millimeter-wave communication antenna needs to operate at 60 or 90 GHz band.
- ➢ Isolation enhancement in MIMO antenna system to improve diversity parameter and overall MIMO performance.
- ➢ Chip antenna design- at millimeter-wave frequency chip antennas are preferred over PCB technology as it introduces high insertion losses from circuit to the antenna. The design of the chip antenna should obey the rules of chip technology. The main challenge in chip antenna design is the low thickness of the substrate and it confines bandwidth and efficiency of the antenna.
- ➢ In antenna design, the gain and bandwidth depend on the size of the antenna. At higher frequencies, this relationship strictly limits the reduction of the physical size of the antenna while concurrently increase bandwidth and radiation efficiency. Therefore there is a considerable challenge in reducing the physical size of the antenna at the same time increasing its bandwidth.
- ➢ MTM based antenna for wearable electronics systems such as health monitoring system, physical training, etc. In the wireless body area network critical component is a wearable antenna for wireless communication.
- ➢ Development of reconfigurable antenna using tunable MTMs.
- ➢ Implanted antenna design for numerous medical applications. Utilization of MTM properties for developing miniaturized and acceptable radiation level implanted antennas.

The presented paper demonstrates the demand for a low profile, compact, high gain, enhanced bandwidth, CP, and highly isolated antenna by utilizing MTM structures in the current and future wireless communication system. Developing a compact antenna having good performance parameters and mutual coupling suppression in MIMO antenna as mentioned above is still challenging. Thus, this review paper will provide an insight to all the antenna researchers in utilizing the exotic properties of MTM in designing high performance antennas to meet the aforementioned challenges.

REFERENCES

[1] L.-H. Wen, S. Gao, C.-X. Mao, Q. Luo, W. Hu, Y. Yin, and X. Yang, "A wideband dual-polarized antenna using shorted dipoles," *IEEE Access*, vol. 6, pp. 39725–39733, 2018.

[2] C. Wang, Y. Chen, and S. Yang, "Dual-band dual-polarized antenna array with flat-top and sharp cutoff radiation patterns for 2G/3G/LTE cellular bands," *IEEE Trans. Antennas Propag.*, vol. 66, no. 11, pp. 5907–5917, Nov. 2018.

[3] G.-F. Cui, S.-G. Zhou, S.-X. Gong, and Y. Liu, "Design of a dual-polarized wideband antenna for 2G/3G/4G mobile communication base station application," *Microw. Opt. Technol. Lett.*, vol. 58, no. 6, pp. 1329–1332, Jun. 2016.

[4] D. Yang, S. Liu, and Z. Zhao, "A broadband dual-polarized printed dipole antenna with low cross-polarization and high isolation for base station applications," *Microw. Opt. Technol. Lett.*, vol. 59, no. 5, pp. 1107–1111, May 2017.

[5] D.-Z. Zheng and Q.-X. Chu, "A wideband dual-polarized antenna with two independently controllable resonant modes and its array for base-station applications," *IEEE Antennas Wireless Propag. Lett.*, vol. 16, pp. 2014–2017, 2017.

[6] C. Wang, Y. Chen, and S. Yang, "Dual-band dual-polarized antenna array with flat-top and sharp cutoff radiation patterns for 2G/3G/LTE cellular bands," *IEEE Trans. Antennas Propag.*, vol. 66, no. 11, pp. 5907–5917, Nov. 2018.

[7] Y. Cui, R. Li, and P. Wang, "Novel dual-broadband planar antenna and its array for 2G/3G/LTE base stations," *IEEE Trans. Antennas Propag.*, vol. 61, no. 3, pp. 1132–1139, Mar. 2013.

[8] Z. Tang, J. Liu, Y.-M. Cai, J. Wang, and Y. Yin, "A wideband differentially fed dual-polarized stacked patch antenna with tuned slot excitations," *IEEE Trans. Antennas Propag.*, vol. 66, no. 4, pp. 2055–2060, Apr. 2018.

[9] H. Huang, X. Li, and Y. Liu, "A novel vector synthetic dipole antenna and its common aperture array," *IEEE Trans. Antennas Propag.*, vol. 66, no. 6, pp. 3183–3188, Jun. 2018.

[10] C. Ding, H.-H. Sun, R. W. Ziolkowski, and Y. Jay Guo, "A dual layered loop array antenna for base stations with enhanced cross-polarization discrimination," *IEEE Trans. Antennas Propag.*, vol. 66, no. 12, pp. 6975–6985, Dec. 2018.

[11] Q. Zhang and Y. Gao, "A compact broadband dual-polarized antenna array for base stations," *IEEE Antennas Wireless Propag. Lett.*, vol. 17, no. 6, pp. 1073–1076, Jun. 2018.

[12] Q.-X. Chu, D.-L. Wen, and Y. Luo, "A broadband ±45° dual-polarized antenna with Y-Shaped feeding lines," *IEEE Trans. Antennas Propag.*, vol. 63, no. 2, pp. 483–490, Feb. 2015.

[13] C. F. Ding, X. Y. Zhang, Y. Zhang, Y. M. Pan, and Q. Xue, "Compact broadband dual-polarized filtering dipole antenna with high selectivity for base-station applications," *IEEE Trans. Antennas Propag.*, vol. 66, no. 11, pp. 5747–5756, Nov. 2018.

[14] Y. Cui, L. Wu, and R. Li, "Bandwidth enhancement of a broadband dual-polarized antenna for 2G/3G/4G and IMT base stations," *IEEE Trans. Antennas Propag.*, vol. 66, no. 12, pp. 7368–7373, Dec. 2018.

[15] Z. Liang, C. Lu, Y. Li, J. Liu, and Y. Long, "A broadband dual-polarized antenna with front-to-back ratio enhancement using semicylindrical sidewalls," *IEEE Trans. Antennas Propag.*, vol. 66, no. 7, pp. 3735–3740, Jul. 2018.

[16] *21st Century Electromagnetics*. Accessed: Jul. 3, 2020. [Online]. Available: https://empossible.net/wp-content/uploads/2020/01/Lecture-Introduction-to-Engineered-Materials.pdf

[17] T. J. Cui, D. R. Smith, and R. Liu, *Metamaterials*. Spring Street, NY, USA: Springer, 2010.

[18] W. Rotman, "Plasma simulation by artificial dielectrics and parallel-plate media," *IRE Trans. Antennas Propag.*, vol. 10, no. 1, pp. 82–95, Jan. 1962.

[19] V. G. Veselago, "The electrodynamics of substances with simultaneously negative values of ϵ and μ," *Sov. Phys. Uspekhi*, vol. 10, no. 4, pp. 509–514, Apr. 1968.

[20] J. B. Pendry, A. J. Holden, W. J. Stewart, and I. Youngs, "Extremely low frequency plasmons in metallic mesostructures," *Phys. Rev. Lett.*, vol. 76, no. 25, pp. 4773–4776, Jun. 1996.

[21] J. B. Pendry, A. J. Holden, D. J. Robbins, and W. J. Stewart, "Magnetism from conductors and enhanced nonlinear phenomena," *IEEE Trans. Microw. Theory Techn.*, vol. 47, no. 11, pp. 2075–2084, 1999.

[22] D. R. Smith, W. J. Padilla, D. C. Vier, S. C. Nemat-Nasser, and S. Schultz, "Composite medium with simultaneously negative permeability and permittivity," *Phys. Rev. Lett.*, vol. 84, no. 18, pp. 4184–4187, May 2000.

[23] R. A. Shelby, "Experimental verification of a negative index of refraction," *Science*, vol. 292, no. 5514, pp. 77–79, Apr. 2001.

[24] H. Nakano, *Low-profile Natural and Metamaterial Antennas: Analysis Methods and Applications*. Hoboken, NJ, USA: Wiley, 2016.

[25] C. Caloz and T. Itoh, *Electromagnetic Metamaterials: Transmission Line Theory and Microwave Applications*. Hoboken, NJ, USA: Wiley, NOV. 2005.

[26] R. Marqués, F. Martin, and M. Sorolla, *Metamaterials With Negative Parameters: Theory, Design, and Microwave Applications*. Hoboken, NJ, USA: Wiley, Sep. 2011.

[27] H. Rother, *Surface Plasmons on Smooth and Rough Surfaces and on Gratings*. New York, NY, USA: Springer-Verlag, 1988.

[28] L. D. Landau and E. M. Lifshitz, *The Classical Theory of Fields*, 4th ed. Oxford, U.K.: Butterworth-Heinemann, 1975.

[29] A. K. Sarychev and V. M. Shalaev, *Electrodynamics of Metamaterials*. Singapore: World Scientific, 2007.

[30] S. I. Maslovski, S. A. Tretyakov, and P. A. Belov, "Wire media with negative effective permittivity: A quasi-static model," *Microw. Opt. Technol. Lett.*, vol. 35, no. 1, pp. 47–51, Oct. 2002.

[31] P. A. Belov, S. A. Tretyakov, and A. J. Viitanen, "Dispersion and reflection properties of artificial media formed by regular lattices of ideally conducting wires," *J. Electromagn. Waves Appl.*, vol. 16, no. 8, pp. 1153–1170, Jan. 2002.

[32] G. J. Long and F. Grandjean, *Supermagnets, Hard Magnetic Materials*. Cham, Switzerland: Springer, Dec. 2012.

[33] W. Cai and V. M. Shalaev, *Optical Metamaterials*. New York, NY, USA: Springer, 2010.

[34] L. D. Landau, J. S. Bell, M. J. Kearsley, L. P. Pitaevskii, E. M. Lifshitz, and J. B. Sykes, *Electrodynamics of Continuous Media*. Amsterdam, The Netherlands: Elsevier, Oct. 2013.

[35] S. A. Schelkunoff and H. T. Friis, *Antennas: Theory and Practice*, 3rd ed. New York, NY, USA: Wiley, 1966.

[36] O. Sydoruk, E. Tatartschuk, E. Shamonina, and L. Solymar, "Analytical formulation for the resonant frequency of split rings," *J. Appl. Phys.*, vol. 105, no. 1, Jan. 2009, Art. no. 014903.

[37] S. S. Eaton, G. R. Eaton, and L. J. Berliner, *Biomedical EPR-Part B: Methodology, Instrumentation, and Dynamics*. Cham, Switzerland: Springer, 2004.

[38] W. N. Hardy and L. A. Whitehead, "Split-ring resonator for use in magnetic resonance from 200–2000 MHz," *Rev. Sci. Instrum.*, vol. 52, no. 2, pp. 213–216, Feb. 1981.

[39] W. Froncisz and J. S. Hyde, "The loop-gap resonator: A new microwave lumped circuit ESR sample structure," *J. Magn. Reson.*, vol. 47, no. 3, pp. 515–521, May 1982.

[40] M. Mehdizadeh and T. K. Ishii, "Electromagnetic field analysis and calculation of the resonance characteristics of the loop-gap resonator," *IEEE Trans. Microw. Theory Techn.*, vol. 37, no. 7, pp. 1113–1118, Jul. 1989.

[41] E. Tatartschuk, N. Gneiding, F. Hesmer, A. Radkovskaya, and E. Shamonina, "Mapping inter-element coupling in metamaterials: Scaling down to infrared," *J. Appl. Phys.*, vol. 111, no. 9, May 2012, Art. no. 094904.

[42] N. Gneiding, O. Zhuromskyy, E. Shamonina, and U. Peschel, "Circuit model optimization of a nano split ring resonator dimer antenna operating in infrared spectral range," *J. Appl. Phys.*, vol. 116, no. 16, Oct. 2014, Art. no. 164311.

[43] C. Saha and J. Y. Siddiqui, "Theoretical model for estimation of resonance frequency of rotational circular split-ring resonators," *Electromagnetics*, vol. 32, no. 6, pp. 345–355, Jul. 2012.

[44] R. Marques, F. Mesa, J. Martel, and F. Medina, "Comparative analysis of edge- and broadside-coupled split ring resonators for metamaterial design–theory and experiments," *IEEE Trans. Antennas Propag.*, vol. 51, no. 10, pp. 2572–2581, Oct. 2003.

[45] D. Ellstein, B. Wang, and K. H. Teo, "Accurate models for spiral resonators," in *Proc. 42nd Eur. Microw. Conf.*, Oct. 2012, pp. 787–790.

[46] F. Bilotti, A. Toscano, and L. Vegni, "Design of spiral and multiple split-ring resonators for the realization of miniaturized metamaterial samples," *IEEE Trans. Antennas Propag.*, vol. 55, no. 8, pp. 2258–2267, Aug. 2007.

[47] J. B. Pendry, A. J. Holden, D. J. Robbins, and W. J. Stewart, "Magnetism from conductors and enhanced nonlinear phenomena," *IEEE Trans. Microw. Theory Techn.*, vol. 47, no. 11, pp. 2075–2084, Nov. 1999.

[48] A. Demetriadou and J. B. Pendry, "Extreme chirality in swiss roll metamaterials," *J. Phys., Condens. Matter*, vol. 21, no. 37, Sep. 2009, Art. no. 376003.

[49] A. Marwaha, "An accurate approach of mathematical modeling of SRR and SR for metamaterials," *J. Eng. Sci. Technol. Rev.*, vol. 9, no. 6, pp. 82–86, Dec. 2016.

[50] F. Bilotti, A. Toscano, and L. Vegni, "Design of spiral and multiple split-ring resonators for the realization of miniaturized metamaterial samples," *IEEE Trans. Antennas Propag.*, vol. 55, no. 8, pp. 2258–2267, Aug. 2007.

[51] S. Bose, M. Ramraj, and S. Raghavan, "Design, analysis and verification of hexagon split ring resonator based negative index metamaterial," in *Proc. Annu. IEEE India Conf. (INDICON)*, Kochi, India, Dec. 2012, pp. 1009–1013.
[52] C. Saha and J. Y. Siddiqui, "A comparative analyis for split ring resonators of different geometrical shapes," in *Proc. IEEE Appl. Electromagn. Conf. (AEMC)*, Kolkata, India, Dec. 2011, pp. 1–4.
[53] F. Miyamaru, S. Kubota, T. Nakanishi, S. Kawashima, N. Sato, M. Kitano, and M. W. Takeda, "Transmission properties of double-gap asymmetric split ring resonators in terahertz region," *Appl. Phys. Lett.*, vol. 101, no. 5, Jul. 2012, Art. no. 051112.
[54] B. Wu, B. Li, T. Su, and C.-H. Liang, "Study on transmission characteristic of split-ring resonator defected ground structure," *PIERS Online*, vol. 2, no. 6, pp. 710–714, 2006.
[55] I. A. I. Al-Naib, C. Jansen, and M. Koch, "Thin-film sensing with planar asymmetric metamaterial resonators," *Appl. Phys. Lett.*, vol. 93, no. 8, Aug. 2008, Art. no. 083507.
[56] M. Kafesaki, T. Koschny, R. S. Penciu, T. F. Gundogdu, E. N. Economou, and C. M. Soukoulis, "Left-handed metamaterials: Detailed numerical studies of the transmission properties," *J. Opt. A, Pure Appl. Opt.*, vol. 7, no. 2, pp. S12–S22, Feb. 2005.
[57] K. Aydin, I. Bulu, K. Guven, M. Kafesaki, C. M. Soukoulis, and E. Ozbay, "Investigation of magnetic resonances for different split-ring resonator parameters and designs," *New J. Phys.*, vol. 7, no. 1, p. 168, 2005.
[58] R. S. Penciu, K. Aydin, M. Kafesaki, T. Koschny, E. Ozbay, E. N. Economou, and C. M. Soukoulis, "Multi-gap individual and coupled split-ring resonator structures," *Opt. Exp.*, vol. 16, no. 22, pp. 18131–18144, 2008.
[59] B. Sauviac, C. R. Simovski, and S. A. Tretyakov, "Double split-ring resonators: Analytical modeling and numerical simulations," *Electromagnetics*, vol. 24, no. 5, pp. 317–338, Jan. 2004.
[60] C. Caloz and T. Itoh, "Application of the transmission line theory of left-handed (LH) materials to the realization of a microstrip 'LH line,"' in *Proc. IEEE Antennas Propag. Soc. Int. Symp.*, San Antonio, TX, USA, 2002, pp. 412–415.
[61] E. J. Rothwell and R. O. Ouedraogo, "Antenna miniaturization: Definitions, concepts, and a review with emphasis on metamaterials," *J. Electromagn. Waves Appl.*, vol. 28, no. 17, pp. 2089–2123, Nov. 2014.
[62] K. Sarabandi, R. Azadegan, H. Mosallaei, and J. Harvey, "Antenna miniaturization techniques for applications in compact wireless transceivers," in *Proc. 27th Gen. Assembly URSI*, Maastricht, The Netherlands, 2002, pp. 1–4.
[63] R. A. Pandhare, P. L. Zade, and M. P. Abegaonkar, "Miniaturized microstrip antenna array using defected ground structure with enhanced performance," *Eng. Sci. Technol., Int. J.*, vol. 19, no. 3, pp. 1360–1367, Sep. 2016.
[64] A. Swetha and K. R. Naidu, "Miniaturized antenna using DGS and meander structure for dual-band application," *Microw. Opt. Technol. Lett.*, vol. 62, no. 11, pp. 3556–3563, Nov. 2020.
[65] K. Han, M. Swaminathan, R. Pulugurtha, H. Sharma, R. Tummala, S. Yang, and V. Nair, "Magneto-dielectric nanocomposite for antenna miniaturization and SAR reduction," *IEEE Antennas Wireless Propag. Lett.*, vol. 15, pp. 72–75, 2016.
[66] S. Kumar and D. K. Vishwakarma, "Miniaturisation of microstrip patch antenna using an artificial planar magneto-dielectric meta-substrate," *IET Microw., Antennas Propag.*, vol. 10, no. 11, pp. 1235–1241, Aug. 2016.
[67] R. Durbha and M. N. Afsar, "Miniaturization techniques using magnetic materials for broadband antenna applications," *IEEE Trans. Magn.*, vol. 55, no. 7, pp. 1–7, Jul. 2019.
[68] D. Bonefačić and J. Bartolić, "Small antennas: Miniaturization techniques and applications," *Automatika*, vol. 53, no. 1, pp. 20–30, Jan. 2012.
[69] B. Xi, Y. Li, and Y. Long, "A miniaturized periodic microstrip leaky wave antenna with shorting pins," *Int. J. Antennas Propag.*, vol. 2019, pp. 1–7, Aug. 2019.
[70] Y. Dong and T. Itoh, "Metamaterial-based antennas," *Proc. IEEE*, vol. 100, no. 7, pp. 2271–2285, Jul. 2012.
[71] L.-Y. Liu and B.-Z. Wang, "A broadband and electrically small planar monopole employing metamaterial transmission line," *IEEE Antennas Wireless Propag. Lett.*, vol. 14, pp. 1018–1021, 2015.
[72] R. W. Ziolkowski and A. Erentok, "Metamaterial-based efficient electrically small antennas," *IEEE Trans. Antennas Propag.*, vol. 54, no. 7, pp. 2113–2130, Jul. 2006.
[73] A. Gupta and R. K. Chaudhary, "A miniaturized dual-band ZOR antenna using epsilon negative transmission line loading," *Int. J. Microw. Wireless Technol.*, vol. 9, no. 8, p. 1735, 2017.
[74] B. R. Gudibandi, H. A. Murugan, and S. K. Dhamodharan, "Miniaturization of monopole antenna using high refractive index metamaterial loading," *Int. J. RF Microw. Comput.-Aided Eng.*, vol. 30, no. 5, May 2020.
[75] S.-T. Ko and J.-H. Lee, "Miniaturized ENG ZOR antenna with high permeability material," in *Proc. IEEE Antennas Propag. Soc. Int. Symp.*, Toronto, ON, Canada, Jul. 2010, pp. 1–4.
[76] E. Irci, K. Sertel, and J. L. Volakis, "Antenna miniaturization for vehicular platforms using printed coupled lines emulating magnetic photonic crystals," *Metamaterials*, vol. 4, nos. 2–3, pp. 127–138, Aug. 2010.
[77] J. Volakis, G. Mumcu, K. Sertel, C.-C. Chen, M. Lee, B. Kramer, D. Psychoudakis, and G. Kiziltas, "Antenna miniaturization using magnetic-photonic and degenerate band-edge crystals," *IEEE Antennas Propag. Mag.*, vol. 48, no. 5, pp. 12–28, Oct. 2006.
[78] J.-H. Park, Y.-H. Ryu, J.-G. Lee, and J.-H. Lee, "Epsilon negative zeroth-order resonator antenna," *IEEE Trans. Antennas Propag.*, vol. 55, no. 12, pp. 3710–3712, Dec. 2007.
[79] S. K. Sharma, A. Gupta, and R. K. Chaudhary, "Epsilon negative CPW-fed zeroth-order resonating antenna with backed ground plane for extended bandwidth and miniaturization," *IEEE Trans. Antennas Propag.*, vol. 63, no. 11, pp. 5197–5203, Nov. 2015.
[80] R. Kumar, R. Singh, and R. K. Chaudhary, "Miniaturised triple-band antenna loaded with complementary concentric closed ring resonators with asymmetric coplanar waveguide-fed based on epsilon negative transmission line," *IET Microw., Antennas Propag.*, vol. 12, no. 13, pp. 2073–2079, Oct. 2018.
[81] M. S. Majedi and A. R. Attari, "Dual-band resonance antennas using epsilon negative transmission line," *IET Microw., Antennas Propag.*, vol. 7, no. 4, pp. 259–267, Mar. 2013.
[82] R. O. Ouedraogo, E. J. Rothwell, A. R. Diaz, K. Fuchi, and A. Temme, "Miniaturization of patch antennas using a metamaterial-inspired technique," *IEEE Trans. Antennas Propag.*, vol. 60, no. 5, pp. 2175–2182, May 2012.
[83] R. K. Saraswat and M. Kumar, "A quad band metamaterial miniaturized antenna for wireless applications with gain enhancement," *Wireless Pers. Commun.*, vol. 114, no. 4, pp. 3595–3612, Oct. 2020.
[84] Z. Troudi, J. Machac, and L. Osman, "Miniaturised planar band-pass filter based on interdigital arm SRR," *IET Microw., Antennas Propag.*, vol. 13, no. 12, pp. 2081–2086, Oct. 2019.
[85] P. H. Rao, J. S. Sajin, and K. Kudesia, "Miniaturisation of switched beam array antenna using phase delay properties of CSRR-loaded transmission line," *IET Microw., Antennas Propag.*, vol. 12, no. 12, pp. 1960–1966, Oct. 2018.
[86] X. Y. Liu, Z. T. Wu, Y. Fan, and E. M. Tentzeris, "A miniaturized CSRR loaded wide-beamwidth circularly polarized implantable antenna for subcutaneous real-time glucose monitoring," *IEEE Antennas Wireless Propag. Lett.*, vol. 16, pp. 577–580, 2017.
[87] M. S. Khan, A.-D. Capobianco, S. M. Asif, D. E. Anagnostou, R. M. Shubair, and B. D. Braaten, "A compact CSRR-enabled UWB diversity antenna," *IEEE Antennas Wireless Propag. Lett.*, vol. 16, pp. 808–812, 2017.
[88] D. Sievenpiper, L. Zhang, R. F. J. Broas, N. G. Alexopolous, and E. Yablonovitch, "High-impedance electromagnetic surfaces with a forbidden frequency band," *IEEE Trans. Microw. Theory Techn.*, vol. 47, no. 11, pp. 2059–2074, Nov. 1999.
[89] D. Sievenpiper, "High-impedance electromagnetic surfaces," Dept. Elect. Eng., Univ. California, Los Angeles, CA, USA, Tech. Rep. 33, 1999.
[90] Y. Zhang, J. von Hagen, M. Younis, C. Fischer, and W. Wiesbeck, "Planar artificial magnetic conductors and patch antennas," *IEEE Trans. Antennas Propag.*, vol. 51, no. 10, pp. 2704–2712, Oct. 2003.
[91] J. Wu and K. Sarabandi, "Reactive impedance surface TM mode slow wave for patch antenna miniaturization [AMTA Corner]," *IEEE Antennas Propag. Mag.*, vol. 56, no. 6, pp. 279–293, Dec. 2014.
[92] S. Jagtap, A. Chaudhari, N. Chaskar, S. Kharche, and R. K. Gupta, "A wideband microstrip array design using RIS and PRS layers," *IEEE Antennas Wireless Propag. Lett.*, vol. 17, no. 3, pp. 509–512, Mar. 2018.
[93] W. Yin, H. Zhang, T. Zhong, and X. Min, "Ultra-miniaturized low-profile angularly-stable frequency selective surface design," *IEEE Trans. Electromagn. Compat.*, vol. 61, no. 4, pp. 1234–1238, Aug. 2019.

[94] M. Yan, S. Qu, J. Wang, J. Zhang, A. Zhang, S. Xia, and W. Wang, "A novel miniaturized frequency selective surface with stable resonance," *IEEE Antennas Wireless Propag. Lett.*, vol. 13, pp. 639–641, 2014.

[95] T. Hong, M. Wang, K. Peng, and S. Gong, "Ultrathin and miniaturized frequency selective surface with closely located dual resonance," *IEEE Antennas Wireless Propag. Lett.*, vol. 18, no. 6, pp. 1288–1292, Jun. 2019.

[96] S. S. Sampath, R. Sivasamy, and K. J. J. Kumar, "A novel miniaturized polarization independent band-stop frequency selective surface," *IEEE Trans. Electromagn. Compat.*, vol. 61, no. 5, pp. 1678–1681, Oct. 2019.

[97] X. Shen, Y. Liu, L. Zhao, G.-L. Huang, X. Shi, and Q. Huang, "A miniaturized microstrip antenna array at 5G millimeter-wave band," *IEEE Antennas Wireless Propag. Lett.*, vol. 18, no. 8, pp. 1671–1675, Aug. 2019.

[98] N. Engheta and R. W. Ziolkowski, Eds., *Metamaterials: Physics and Engineering Explorations*. Hoboken, NJ, USA: Wiley, 2006.

[99] G. Varamini, A. Keshtkar, and M. Naser-Moghadasi, "Compact and miniaturized microstrip antenna based on fractal and metamaterial loads with reconfigurable qualification," *AEU-Int. J. Electron. Commun.*, vol. 83, pp. 213–221, Jan. 2018.

[100] M. Alibakhshi-Kenari, M. Naser-Moghadasi, R. A. Sadeghzadeh, B. S. Virdee, and E. Limiti, "Miniature CRLH-based ultra wideband antenna with gain enhancement for wireless communication applications," *ICT Exp.*, vol. 2, no. 2, pp. 75–79, Jun. 2016.

[101] A. Jafargholi and A. Jafargholi, "Miniaturisation of printed slot antennas using artificial magnetic conductors," *IET Microw., Antennas Propag.*, vol. 12, no. 7, pp. 1054–1059, Jun. 2018.

[102] T. Shaw and D. Mitra, "Efficient design of electrically small antenna using metamaterials for wireless applications," *CSI Trans. ICT*, vol. 6, no. 1, pp. 51–58, Mar. 2018.

[103] A. Gupta and R. K. Singh, "A miniaturized elliptically shaped split ring resonator antenna with dual-band characteristics," in *Advances in Signal Processing and Communication*. Singapore: Springer, 2019, pp. 37–44.

[104] Z. Wang, Y. Dong, and T. Itoh, "Miniaturized wideband CP antenna based on metaresonator and CRLH-TLs for 5G new radio applications," *IEEE Trans. Antennas Propag.*, vol. 69, no. 1, pp. 74–83, Jan. 2021.

[105] M. Nabil and M. M. A. Faisal, "Design, simulation and analysis of a high gain small size array antenna for 5G wireless communication," *Wireless Pers. Commun.*, pp. 1–16, Sep. 2020, doi: 10.1007/s11277-020-07819-9.

[106] G. Augustin, Q. Rao, and T. A. Denidni, "Low-profile antennas," in *Handbook of Antenna Technologies*, Z. Chen, D. Liu, H. Nakano, X. Qing, and T. Zwick, Eds. Singapore: Springer, 2016.

[107] Nasimuddin and K. P. Esselle, "A low-profile compact microwave antenna with high gain and wide bandwidth," *IEEE Trans. Antennas Propag.*, vol. 55, no. 6, pp. 1880–1883, Jun. 2007.

[108] Z. Wang and J. A. Liu, "A compact directional microstrip antenna with wide bandwidth, high gain, and high front-to-back ratio," *Microw. Opt. Technol. Lett.*, vol. 62, no. 1, pp. 308–314, Jan. 2020.

[109] J. Wang, Q. Liu, and L. Zhu, "Bandwidth enhancement of a differential-fed equilateral triangular patch antenna via loading of shorting posts," *IEEE Trans. Antennas Propag.*, vol. 65, no. 1, pp. 36–43, Jan. 2017.

[110] A. Katyal and A. Basu, "Compact and broadband stacked microstrip patch antenna for target scanning applications," *IEEE Antennas Wireless Propag. Lett.*, vol. 16, pp. 381–384, 2017.

[111] K. D. Xu, H. Xu, Y. Liu, J. Li, and Q. H. Liu, "Microstrip patch antennas with multiple parasitic patches and shorting vias for bandwidth enhancement," *IEEE Access*, vol. 6, pp. 11624–11633, 2018.

[112] K. Mandal and P. P. Sarkar, "A compact low profile wideband U-shape antenna with slotted circular ground plane," *AEU-Int. J. Electron. Commun.*, vol. 70, no. 3, pp. 336–340, Mar. 2016.

[113] M. Alibakhshi-Kenari, M. Naser-Moghadasi, R. A. Sadeghzadeh, B. S. Virdee, and E. Limiti, "Bandwidth extension of planar antennas using embedded slits for reliable multiband RF communications," *AEU-Int. J. Electron. Commun.*, vol. 70, no. 7, pp. 910–919, Jul. 2016.

[114] B. Yuan, Y. H. Zheng, X. H. Zhang, B. You, and G. Q. Luo, "A bandwidth and gain enhancement for microstrip antenna based on metamaterial," *Microw. Opt. Technol. Lett.*, vol. 59, no. 12, pp. 3088–3093, Dec. 2017.

[115] B. Urul, "Gain enhancement of microstrip antenna with a novel DNG material," *Microw. Opt. Technol. Lett.*, vol. 62, no. 4, pp. 1824–1829, Apr. 2020.

[116] R. W. Ziolkowski and A. D. Kipple, "Application of double negative materials to increase the power radiated by electrically small antennas," *IEEE Trans. Antennas Propag.*, vol. 51, no. 10, pp. 2626–2640, Oct. 2003.

[117] Y. M. Pan and S. Y. Zheng, "A low-profile stacked dielectric resonator antenna with high-gain and wide bandwidth," *IEEE Antennas Wireless Propag. Lett.*, vol. 15, pp. 68–71, 2016.

[118] M. M. Moeini, H. Oraizi, A. Amini, and V. Nayyeri, "Wide-band beam-scanning by surface wave confinement on leaky wave holograms," *Sci. Rep.*, vol. 9, no. 1, pp. 1–11, Dec. 2019.

[119] T. D. Amalraj and R. Savarimuthu, "Design and analysis of microstrip antenna on periodic and non-periodic photonic band gap substrate," *IETE J. Res.*, pp. 1–10, Jul. 2020, doi: 10.1080/03772063.2020.1791744.

[120] P. Jin, C.-C. Lin, and R. W. Ziolkowski, "Multifunctional, electrically small, planar near-field resonant parasitic antennas," *IEEE Antennas Wireless Propag. Lett.*, vol. 11, pp. 200–204, 2012.

[121] N. Zhu and R. W. Ziolkowski, "Active metamaterial-inspired broad-bandwidth, efficient, electrically small antennas," *IEEE Antennas Wireless Propag. Lett.*, vol. 10, pp. 1582–1585, 2011.

[122] D. Chen, H. Zhang, and C. Zhao, "A novel printed monopole antenna with stepped impedance hairpin resonator loading," *IEEE Access*, vol. 8, pp. 96975–96980, 2020.

[123] X. Chen, M.-C. Tang, D. Yi, and R. W. Ziolkowski, "Wideband, electrically small, near-field resonant parasitic dipole antenna with stable radiation performance," *IEEE Antennas Wireless Propag. Lett.*, vol. 19, no. 5, pp. 826–830, May 2020.

[124] R. Pandeeswari and S. Raghavan, "Microstrip antenna with complementary split ring resonator loaded ground plane for gain enhancement," *Microw. Opt. Technol. Lett.*, vol. 57, no. 2, pp. 292–296, Feb. 2015.

[125] W. Cao, W. Ma, W. Peng, and Z. N. Chen, "Bandwidth-enhanced electrically large microstrip antenna loaded with SRR structures," *IEEE Antennas Wireless Propag. Lett.*, vol. 18, no. 4, pp. 576–580, Apr. 2019.

[126] S. K. Patel and C. Argyropoulos, "Enhanced bandwidth and gain of compact microstrip antennas loaded with multiple corrugated split ring resonators," *J. Electromagn. Waves Appl.*, vol. 30, no. 7, pp. 945–961, May 2016.

[127] Z. Wang, Y. Dong, and T. Itoh, "Ultraminiature circularly polarized RFID antenna inspired by crossed split-ring resonator," *IEEE Trans. Antennas Propag.*, vol. 68, no. 6, pp. 4196–4207, Jun. 2020.

[128] J. Wang, H. Wong, Z. Ji, and Y. Wu, "Broadband CPW-fed aperture coupled metasurface antenna," *IEEE Antennas Wireless Propag. Lett.*, vol. 18, no. 3, pp. 517–520, Mar. 2019.

[129] T. Wu, J. Chen, and P.-F. Wu, "Broadband and multi-mode Fabry–Pérot cavity antenna with gain enhancement," *AEU-Int. J. Electron. Commun.*, vol. 127, Dec. 2020, Art. no. 153440.

[130] F. Yang and Y. Rahmat-Samii, *Electromagnetic Band Gap Structures in Antenna Engineering*. Cambridge, U.K.: Cambridge Univ. Press, 2010.

[131] P. Sambandam, M. Kanagasabai, S. Ramadoss, R. Natarajan, M. G. N. Alsath, S. Shanmuganathan, M. Sindhadevi, and S. K. Palaniswamy, "Compact monopole antenna backed with fork-slotted EBG for wearable applications," *IEEE Antennas Wireless Propag. Lett.*, vol. 19, no. 2, pp. 228–232, Feb. 2020.

[132] P. K. Panda and D. Ghosh, "Wideband and high gain tuning fork shaped monopole antenna using high impedance surface," *AEU-Int. J. Electron. Commun.*, vol. 111, Nov. 2019, Art. no. 152920.

[133] S. Narayan, B. Sangeetha, and R. M. Jha, *Frequency Selective Surfaces based High Performance Microstrip Antenna*. Singapore: Springer, 2016, pp. 1–40.

[134] J. Zhu, S. Li, S. Liao, and Q. Xue, "Wideband low-profile highly isolated MIMO antenna with artificial magnetic conductor," *IEEE Antennas Wireless Propag. Lett.*, vol. 17, no. 3, pp. 458–462, Mar. 2018.

[135] R. Sonak, M. Ameen, and R. K. Chaudhary, "High gain dual-band open-ended metamaterial antenna utilizing CRR with broadside radiation characteristics based on left-handed AMC and PEC," *Mater. Res. Exp.*, vol. 6, no. 5, Feb. 2019, Art. no. 055811.

[136] T. Jang, J. Choi, and S. Lim, "Compact coplanar waveguide (CPW)-fed zeroth-order resonant antennas with extended bandwidth and high efficiency on vialess single layer," *IEEE Trans. Antennas Propag.*, vol. 59, no. 2, pp. 363–372, Feb. 2011.

[137] P.-W. Chen and F.-C. Chen, "Asymmetric coplanar waveguide (ACPW) zeroth-order resonant (ZOR) antenna with high efficiency and bandwidth enhancement," *IEEE Antennas Wireless Propag. Lett.*, vol. 11, pp. 527–530, 2012.

[138] B.-J. Niu, Q.-Y. Feng, and P.-L. Shu, "Epsilon negative Zeroth- and first-order resonant antennas with extended bandwidth and high efficiency," *IEEE Trans. Antennas Propag.*, vol. 61, no. 12, pp. 5878–5884, Dec. 2013.

[139] P.-L. Chi and Y.-S. Shih, "Compact and bandwidth-enhanced zeroth-order resonant antenna," *IEEE Antennas Wireless Propag. Lett.*, vol. 14, pp. 285–288, 2015.
[140] J. K. Ji, G. H. Kim, and W. M. Seong, "Bandwidth enhancement of metamaterial antennas based on composite right/left-handed transmission line," *IEEE Antennas Wireless Propag. Lett.*, vol. 9, pp. 36–39, 2010.
[141] S. Kumar and R. Kumari, "Composite right/left-handed ultra-wideband metamaterial antenna with improved gain," *Microw. Opt. Technol. Lett.*, vol. 63, no. 1, pp. 188–195, Jan. 2021.
[142] S. Kumar and R. Kumari, "Bandwidth enhanced coplanar waveguide-fed composite right/left handed antenna loaded with resonating rings," *IET Microw., Antennas Propag.*, vol. 13, no. 12, pp. 2134–2140, Oct. 2019.
[143] H. Lee, D.-J. Woo, and S. Nam, "Compact and bandwidth-enhanced asymmetric coplanar waveguide (ACPW) antenna using CRLH-TL and modified ground plane," *IEEE Antennas Wireless Propag. Lett.*, vol. 15, pp. 810–813, 2016.
[144] S. Ahdi Rezaeieh, M. A. Antoniades, and A. M. Abbosh, "Bandwidth and directivity enhancement of loop antenna by nonperiodic distribution of mu-negative metamaterial unit cells," *IEEE Trans. Antennas Propag.*, vol. 64, no. 8, pp. 3319–3329, Aug. 2016.
[145] N. L. Nguyen and V. Y. Vu, "Gain enhancement for MIMO antenna using metamaterial structure," *Int. J. Microw. Wireless Technol.*, vol. 11, no. 08, pp. 851–862, Oct. 2019.
[146] M. Labidi and F. Choubani, "Performances enhancement of metamaterial loop antenna for terahertz applications," *Opt. Mater.*, vol. 82, pp. 116–122, Aug. 2018.
[147] M. Zada, I. A. Shah, and H. Yoo, "Metamaterial-loaded compact high-gain dual-band circularly polarized implantable antenna system for multiple biomedical applications," *IEEE Trans. Antennas Propag.*, vol. 68, no. 2, pp. 1140–1144, Feb. 2020.
[148] S. Ahdi Rezaeieh, M. A. Antoniades, and A. M. Abbosh, "Gain enhancement of wideband metamaterial-loaded loop antenna with tightly coupled arc-shaped directors," *IEEE Trans. Antennas Propag.*, vol. 65, no. 4, pp. 2090–2095, Apr. 2017.
[149] D. Mitra, B. Ghosh, A. Sarkhel, and S. R. Bhadra Chaudhuri, "A miniaturized ring slot antenna design with enhanced radiation characteristics," *IEEE Trans. Antennas Propag.*, vol. 64, no. 1, pp. 300–305, Jan. 2016.
[150] C. Arora, S. S. Pattnaik, and R. N. Baral, "Performance enhancement of patch antenna array for 5.8 GHz wi-MAX applications using metamaterial inspired technique," *AEU-Int. J. Electron. Commun.*, vol. 79, pp. 124–131, Sep. 2017.
[151] M. A. Meriche, H. Attia, A. Messai, S. S. I. Mitu, and T. A. Denidni, "Directive wideband cavity antenna with single-layer meta-superstrate," *IEEE Antennas Wireless Propag. Lett.*, vol. 18, no. 9, pp. 1771–1774, Sep. 2019.
[152] R. Chopra and G. Kumar, "Compact, broadband, and high gain directional endfire antenna," *Microw. Opt. Technol. Lett.*, vol. 62, no. 7, pp. 2546–2553, Jul. 2020.
[153] A. Verma, A. K. Singh, N. Srivastava, S. Patil, and B. K. Kanaujia, "Hexagonal ring electromagnetic band gap-based slot antenna for circular polarization and performance enhancement," *Microw. Opt. Technol. Lett.*, vol. 62, no. 7, pp. 2576–2587, Jul. 2020.
[154] V. R. Nuthakki and S. Dhamodharan, "Via-less CRLH-TL unit cells loaded compact and bandwidth-enhanced metamaterial based antennas," *AEU-Int. J. Electron. Commun.*, vol. 80, pp. 48–58, Oct. 2017.
[155] S. S. Gao, Q. Luo, and F. Zhu, *Circularly Polarized Antennas*. Hoboken, NJ, USA: Wiley, 2013.
[156] S. W. Lee and Y. J. Sung, "Simple polarization reconfigurable antenna with t-shaped feed," *IEEE Antennas Wireless Propag. Lett.*, vol. 15, pp. 114–177, May 2015.
[157] Z.-X. Yang, H.-C. Yang, J.-S. Hong, and Y. Li, "Bandwidth enhancement of a polarization-reconfigurable patch antenna with stair-slots on the ground," *IEEE Antennas Wireless Propag. Lett.*, vol. 13, pp. 579–582, 2014.
[158] X.-X. Yang, B.-C. Shao, F. Yang, A. Z. Elsherbeni, and B. Gong, "A polarization reconfigurable patch antenna with loop slots on the ground plane," *IEEE Antennas Wireless Propag. Lett.*, vol. 11, pp. 69–72, Jan. 2012.
[159] W. Lin and H. Wong, "Wideband circular polarization reconfigurable antenna," *IEEE Trans. Antennas Propag.*, vol. 63, no. 12, pp. 5938–5944, Dec. 2015.
[160] J. Hu, Z.-C. Hao, and W. Hong, "Design of a wideband quad-polarization reconfigurable patch antenna array using a stacked structure," *IEEE Trans. Antennas Propag.*, vol. 65, no. 6, pp. 3014–3023, Jun. 2017.
[161] Y.-M. Cai, S. Gao, Y. Yin, W. Li, and Q. Luo, "Compact-size low-profile wideband circularly polarized omnidirectional patch antenna with reconfigurable polarizations," *IEEE Trans. Antennas Propag.*, vol. 64, no. 5, pp. 2016–2021, May 2016.
[162] K. X. Wang and H. Wong, "A reconfigurable CP/LP antenna with cross-probe feed," *IEEE Antennas Wireless Propag. Lett.*, vol. 16, pp. 669–672, 2017.
[163] L. Ge, X. Yang, D. Zhang, M. Li, and H. Wong, "Polarization-reconfigurable magnetoelectric dipole antenna for 5G Wi-Fi," *IEEE Antennas Wireless Propag. Lett.*, vol. 16, pp. 1504–1507, 2017.
[164] L. Zhang, S. Gao, Q. Luo, P. R. Young, and Q. Li, "Wideband loop antenna with electronically switchable circular polarization," *IEEE Antennas Wireless Propag. Lett.*, vol. 16, pp. 242–245, 2017.
[165] P. Jin and R. W. Ziolkowski, "Multi-frequency, linear and circular polarized, metamaterial-inspired, near-field resonant parasitic antennas," *IEEE Trans. Antennas Propag.*, vol. 59, no. 5, pp. 1446–1459, May 2011.
[166] M.-C. Tang and R. W. Ziolkowski, "Frequency-agile, efficient, circularly polarized, near-field resonant antenna: Designs and measurements," *IEEE Trans. Antennas Propag.*, vol. 63, no. 11, pp. 5203–5209, Nov. 2015.
[167] G. B. Reddy, M. H. Adhithya, and D. S. Kumar, "Design of circularly polarized patch antennas using anisotropic high refractive index metamaterial loading," *Electromagnetics*, vol. 40, no. 3, pp. 98–186, Apr. 2020.
[168] M. Venkateswara Rao, B. T. P. Madhav, T. Anilkumar, and B. P. Nadh, "Metamaterial inspired quad band circularly polarized antenna for WLAN/ISM/Bluetooth/WiMAX and satellite communication applications," *AEU-Int. J. Electron. Commun.*, vol. 97, pp. 229–241, Dec. 2018.
[169] P. K. T. Rajanna, K. Rudramuni, and K. Kandasamy, "A high-gain circularly polarized antenna using zero-index metamaterial," *IEEE Antennas Wireless Propag. Lett.*, vol. 18, no. 6, pp. 1129–1133, Jun. 2019.
[170] J. Chatterjee, A. Mohan, and V. Dixit, "Broadband circularly polarized H-Shaped patch antenna using reactive impedance surface," *IEEE Antennas Wireless Propag. Lett.*, vol. 17, no. 4, pp. 625–628, Apr. 2018.
[171] L.-Y. Liu and B.-Z. Wang, "Compact broadband linearly and circularly polarized antenna based on CRLH transmission line," in *Proc. Asia–Pacific Microw. Conf. (APMC)*, Nanjing, China, Dec. 2015, pp. 1–3.
[172] Z. Wang, Y. Dong, and T. Itoh, "Miniaturized wideband CP antenna based on metaresonator and CRLH-TLs for 5G new radio applications," *IEEE Trans. Antennas Propag.*, vol. 69, no. 1, pp. 74–83, Jan. 2021, doi: 10.1109/TAP.2020.3008626.
[173] P. Liu, W. Jiang, S. Sun, Y. Xi, and S. Gong, "Broadband and low-profile penta-polarization reconfigurable metamaterial antenna," *IEEE Access*, vol. 8, pp. 21823–21831, 2020.
[174] M. A. Sofi, K. Saurav, and S. K. Koul, "Frequency-selective surface-based compact single substrate layer dual-band transmission-type linear-to-circular polarization converter," *IEEE Trans. Microw. Theory Techn.*, vol. 68, no. 10, pp. 4138–4149, Oct. 2020.
[175] Q. Zheng, C. Guo, G. A. E. Vandenbosch, and J. Ding, "Low-profile circularly polarized array with gain enhancement and RCS reduction using polarization conversion EBG structures," *IEEE Trans. Antennas Propag.*, vol. 68, no. 3, pp. 2440–2445, Mar. 2020.
[176] S. X. Ta and I. Park, "Low-profile broadband circularly polarized patch antenna using metasurface," *IEEE Trans. Antennas Propag.*, vol. 63, no. 12, pp. 5929–5934, Dec. 2015.
[177] S. Liu, D. Yang, and J. Pan, "A low-profile broadband dual-circularly-polarized metasurface antenna," *IEEE Antennas Wireless Propag. Lett.*, vol. 18, no. 7, pp. 1395–1399, Jul. 2019.
[178] W. Chaihongsa, R. Kuse, K. Furuya, C. Phongcharoenpanich, and T. Fukusako, "Broadband linear-to-circular polarisation conversion using the diamond-shaped reflecting metasurface," *IET Microw., Antennas Propag.*, vol. 14, no. 9, pp. 943–949, Jul. 2020.
[179] A. R. Vaidya, R. K. Gupta, S. K. Mishra, and J. Mukherjee, "Right-hand/left-hand circularly polarized high-gain antennas using partially reflective surfaces," *IEEE Antennas Wireless Propag. Lett.*, vol. 13, pp. 431–434, 2014.
[180] H. Yi and S.-W. Qu, "A novel dual-band circularly polarized antenna based on electromagnetic band-gap structure," *IEEE Antennas Wireless Propag. Lett.*, vol. 12, pp. 1149–1152, 2013.
[181] R. Liu, X. An, H. Zheng, M. Wang, Z. Gao, and E. Li, "Neutralization line decoupling tri-band multiple-input multiple-output antenna design," *IEEE Access*, vol. 8, pp. 27018–27026, 2020.

[182] G. Srivastava and A. Mohan, "Compact MIMO slot antenna for UWB applications," *IEEE Antennas Wireless Propag. Lett.*, vol. 15, pp. 1057–1060, 2016.

[183] L. Wang, Z. Du, H. Yang, R. Ma, Y. Zhao, X. Cui, and X. Xi, "Compact UWB MIMO antenna with high isolation using fence-type decoupling structure," *IEEE Antennas Wireless Propag. Lett.*, vol. 18, no. 8, pp. 1641–1645, Aug. 2019.

[184] J. Banerjee, A. Karmakar, R. Ghatak, and D. R. Poddar, "Compact CPW-fed UWB MIMO antenna with a novel modified minkowski fractal defected ground structure (DGS) for high isolation and triple band-notch characteristic," *J. Electromagn. Waves Appl.*, vol. 31, no. 15, pp. 1550–1565, Oct. 2017.

[185] M. M. Hassan, M. Rasool, M. U. Asghar, Z. Zahid, A. A. Khan, I. Rashid, A. Rauf, and F. A. Bhatti, "A novel UWB MIMO antenna array with band notch characteristics using parasitic decoupler," *J. Electromagn. Waves Appl.*, vol. 34, no. 9, pp. 1225–1238, Jun. 2020.

[186] L. Wu, Y. Xia, X. Cao, and Z. Xu, "A miniaturized UWB-MIMO antenna with quadruple band-notched characteristics," *Int. J. Microw. Wireless Technol.*, vol. 10, no. 8, pp. 948–955, Oct. 2018.

[187] G. Zhai, Z. N. Chen, and X. Qing, "Enhanced isolation of a closely spaced four-element MIMO antenna system using metamaterial mushroom," *IEEE Trans. Antennas Propag.*, vol. 63, no. 8, pp. 3362–3370, Aug. 2015.

[188] R. Mark, H. V. Singh, K. Mandal, and S. Das, "Mutual coupling reduction using near-zero ϵ and μ metamaterial-based superstrate for an MIMO application," *IET Microw., Antennas Propag.*, vol. 14, no. 6, pp. 479–484, May 2020.

[189] M. Li, B. G. Zhong, and S. W. Cheung, "Isolation enhancement for MIMO patch antennas using near-field resonators as coupling-mode transducers," *IEEE Trans. Antennas Propag.*, vol. 67, no. 2, pp. 755–764, Feb. 2019.

[190] V. Najafy and M. Bemani, "Mutual-coupling reduction in triple-band MIMO antennas for WLAN using CSRRs," *Int. J. Microw. Wireless Technol.*, vol. 12, no. 8, pp. 762–768, Oct. 2020.

[191] M. U. Khan and M. S. Sharawi, "Isolation improvement using an MTM inspired structure with a patch based MIMO antenna system," in *Proc. 8th Eur. Conf. Antennas Propag. (EuCAP)*, The Hague, The Netherlands, Apr. 2014, pp. 2718–2722.

[192] Z. Liu, J. Wang, S. Qu, J. Zhang, H. Ma, Z. Xu, and A. Zhang, "Enhancing isolation of antenna arrays by simultaneously blocking and guiding magnetic field lines using magnetic metamaterials," *Appl. Phys. Lett.*, vol. 109, no. 15, Oct. 2016, Art. no. 153505.

[193] P. Yang, J. Wang, Y. Han, Y. Fan, Y. Li, J. Zhang, and S. Qu, "Harmonic interference suppression within a multiple-antenna system using integrated slender magnetic metamaterials," *Microw. Opt. Technol. Lett.*, vol. 62, no. 1, pp. 355–362, Jan. 2020.

[194] X. Tan, W. Wang, Y. Wu, Y. Liu, and A. A. Kishk, "Enhancing isolation in dual-band meander-line multiple antenna by employing split EBG structure," *IEEE Trans. Antennas Propag.*, vol. 67, no. 4, pp. 2769–2774, Apr. 2019.

[195] M. Alibakhshikenari, M. Khalily, B. S. Virdee, C. H. See, R. A. Abd-Alhameed, and E. Limiti, "Mutual coupling suppression between two closely placed microstrip patches using EM-bandgap metamaterial fractal loading," *IEEE Access*, vol. 7, pp. 23606–23614, 2019.

[196] S. R. Thummaluru, R. Kumar, and R. K. Chaudhary, "Isolation enhancement and radar cross section reduction of MIMO antenna with frequency selective surface," *IEEE Trans. Antennas Propag.*, vol. 66, no. 3, pp. 1595–1600, Mar. 2018.

[197] T. Hassan, M. U. Khan, H. Attia, and M. S. Sharawi, "An FSS based correlation reduction technique for MIMO antennas," *IEEE Trans. Antennas Propag.*, vol. 66, no. 9, pp. 4900–4905, Sep. 2018.

[198] M. Akbari, M. M. Ali, M. Farahani, A. R. Sebak, and T. Denidni, "Spatially mutual coupling reduction between CP-MIMO antennas using FSS superstrate," *Electron. Lett.*, vol. 53, no. 8, pp. 516–518, Apr. 2017.

[199] H. Luan, C. Chen, W. Chen, L. Zhou, H. Zhang, and Z. Zhang, "Mutual coupling reduction of closely E/H-plane coupled antennas through metasurfaces," *IEEE Antennas Wireless Propag. Lett.*, vol. 18, no. 10, pp. 1996–2000, Oct. 2019.

[200] A. A. Ibrahim and M. A. Abdalla, "CRLH MIMO antenna with reversal configuration," *AEU-Int. J. Electron. Commun.*, vol. 70, no. 9, pp. 1134–1141, Sep. 2016.

[201] T. Shabbir, R. Saleem, S. S. Al-Bawri, M. F. Shafique, and M. T. Islam, "Eight-port metamaterial loaded UWB-MIMO antenna system for 3D system-in-package applications," *IEEE Access*, vol. 8, pp. 106982–106992, 2020.

[202] M. H. D. V. K. Reddy Sheela and A. Parbot Sharma, "A compact metamaterial inspired UWB-MIMO fractal antenna with reduced mutual coupling," *Microsyst. Technol.*, pp. 1–13, Sep. 2020, doi: 10.1007/s00542-020-05024-z.

[203] G. Irene and A. Rajesh, "A dual-polarized UWB–MIMO antenna with IEEE 802.11ac band-notched characteristics using split-ring resonator," *J. Comput. Electron.*, vol. 17, no. 3, pp. 1090–1098, Sep. 2018.

[204] J. Ghosh and D. Mitra, "A technique for reduction of mutual coupling by steering surface wave propagation," *Microw. Opt. Technol. Lett.*, vol. 62, no. 5, pp. 1957–1963, May 2020.

[205] X. Zhu, X. Yang, Q. Song, and B. Lui, "Compact UWB-MIMO antenna with metamaterial FSS decoupling structure," *EURASIP J. Wireless Commun. Netw.*, vol. 2017, no. 1, p. 115, Dec. 2017.

[206] E. Thakur, N. Jaglan, and S. D. Gupta, "Design of compact triple band-notched UWB MIMO antenna with TVC-EBG structure," *J. Electromagn. Waves Appl.*, vol. 34, no. 11, pp. 1601–1615, Jul. 2020.

PRAVEEN KUMAR received the B.E. degree in electronics and communication engineering and the M.Tech. degree in microelectronics and control systems from Visvesvaraya Technological University, Belagavi, India. He is currently pursuing the Ph.D. degree with the Department of Electronics and Communication Engineering, Manipal Institute of Technology, Manipal Academy of Higher Education, Manipal, India. His research interest includes microstrip antennas. He is a member of IETE, India.

TANWEER ALI (Senior Member, IEEE) is currently working as an Assistant Professor-Senior Scale with the Department of Electronics and Communication Engineering, Manipal Institute of Technology, Manipal Academy of Higher Education, Manipal. He is an Active Researcher in the field of microstrip antennas, wireless communication, and microwave imaging. He has published more than 97 papers in reputed peer reviewed international journal and conferences. He is an Associate Member of IETE India. He is on the board of reviewers of journals, like the IEEE TRANSACTIONS ON ANTENNAS AND PROPAGATION, IEEE ANTENNAS AND WIRELESS PROPAGATION LETTERS, IEEE ACCESS, *IET Microwaves, Antennas* and *Propagation*, *Electronics Letter* (IET), *Wireless Personal Communications* (WPCs) (Springer), *AEU-International Journal of Electronics and Communications*, *Microwave and Optical Technology Letters* (MOTL) (Wiley), *International Journal of Antennas and Propagation* (Hindawi), *Advanced Electromagnetics*, *Progress in Electromagnetics Research* (PIER), *KSII Transactions on Engineering Science*, *International Journal of Microwave and Wireless Technologies*, *Frequency*, and *Radioengineering*.

M. M. MANOHARA PAI (Senior Member, IEEE) received the Ph.D. degree in computer science and engineering from the Department of Information and Communication Technology, Manipal Institute of Technology, Manipal Academy of Higher Education, Manipal, India, where he has been a Professor for the last 29 years. He holds six patents to his credit and has published 92 articles in national and international journals/conference proceedings. He has published two books and guided five Ph.D.'s and 65 master theses. His research interests include data analytics, cloud computing, the IoT, computer networks, mobile computing, scalable video coding, and robot motion planning. He is a Life Member of ISTE and of Systems Society of India. He is also the Chair of the IEEE Mangalore SubSection, in 2019.